Predicting Climate Induced Changes in the Shallow Groundwater

How do Differently Scaled Hydrological Models Impact the Predictions

Luc Taliesin Eisenbrückner

Water and Environmental Engineering, 2020-06

Master's Project

STUDENT REPORT

AALBORG UNIVERSITY

Predicting Climate Induced Changes in the Shallow Groundwater

How do Differently Scaled Hydrological Models Impact the Predictions

Luc Taliesin Eisenbrückner

Water and Environmental Engineering, 2020-06

Master's Project

STUDENT REPORT

AALBORG UNIVERSITY

Software used in this project: MikeShe and MikeHydro 2019 sp. 1 by DHI, ArcMap 10.5 by Esri, PEST v. 17, Python 3.8.2, ParaView 5.8.0 and Microsoft Excel .

Department of the Built Environment
Aalborg University
http://www.aau.dk

AALBORG UNIVERSITY
STUDENT REPORT

Title:
Predicting Climate Induced Changes in the Shallow Groundwater: How do Differently Scaled Hydrological Models Impact the Predictions

Theme:
Groundwater modeling, shallow groundwater, climate predictions, model scaling, inverse calibration

Project Period:
Spring Semester 2020

Participant:
Luc Taliesin Eisenbrückner

Supervisors:
Søren Liedtke Thorndahl
Niels Claes
Jacob Kidmose, GEUS

Copies: 1

Page Numbers: 57

Date of Completion:
June 10, 2020

Abstract:

Three differently scaled hydrological models are used to predict the climate change induced impact on the shallow groundwater in a local study site in central Jutland. The goal is to test, if the National Water Resources Model for Denmark can be used to predict climate change impacts on the shallow groundwater on a local scale. To test this, a local model with an updated geology and a refined grid was calibrated, focusing on precisely predicting groundwater heads and their variations. The local model predicted larger changes in the shallow groundwater compared to the two other models used. Also the risk assessment in regard to groundwater flooding showed, that the local model predicted the largest areas exposed to groundwater flooding. Those results could maybe be connected to the updated geology in the local model, compared to the other models, but this assumption needs further verification.

Contents

Sammenfatning

Under dette projekt er der anvendt tre forskelligt skalerede numeriske hydrologiske modeller til at forudsige klimaforændringernes påvirkning af det terrænnære grundvand i et lokalt område i Midtjylland. Formålet med undersøgelsen er, at undersøge Danmarks Nationale Vandressource Model kan anvendes til at forudsige klimaforændringernes påvirkning af det terrænnære grundvand på en lokal plan. For at teste dette, er der blevet kalibreret en lokalmodel, med opdateret geologi og forfinet gridstørrelse, til at simulere de nuværende grundvandsforhold så præcist som muligt. Den kalibrerede lokalmodel viste større variationer i påvirkningen af klimaet på det terrænnære grundvand end de andre to anvendte modeller. Der blev også gennemført en risikoanalyse af oversvømmelsesrisici i området. Også her viste lokalmodellen de største områder der var påvirket af grundvandsoversvømmelser. Det tyder på, at den ændrede geologi er den hovedsaglige grund til disse resultater. Dette kræver dog flere undersøgelser at påvise.

Preface

This project is conducted as part of the Masters in Water and Environmental Engineering at Aalborg University under the supervision of Søren Liedtke Thorndahl and Niels Claes. The project was carried out in close collaboration with the Hydrological Department at GEUS, the Geological Survey of Denmark and Greenland, where Jacob Kidmose was my leading supervisor. I want to thank my supervisors for the guidance throughout the process, especially in these strange times of Corona. A special thanks to Jacob Kidmose, Per Rasmussen and Torben O. Sonnenborg for your guidance and sparring in carrying out the calibration. Credits to Jacob Kidmose for the front page picture.

Aalborg University, June 10, 2020

Luc Taliesin Eisenbrückner
leisen18@student.aau.dk

Chapter 1

Introduction

Predicting climate change impacts correctly is a key factor in developing and designing climate change adaption strategies to mitigate the impacts of climate change [7]. It is therefore important to establish models which can use the always improving climate models to predict the impact of the changing climate on the environment [7]. Many countries are interested in nationwide climate change assessments, but lack of data availability and modeling capacities make it difficult to conduct those studies. Especially in the impact of climate change on groundwater it is challenging to predict the climate change effects on the groundwater reliable. One of the difficulties connected to the modeling of climate change impacts on groundwater, is that the groundwater responds slowly to a changing climate [8]. Therefore, long simulation periods are needed, and sufficient data is required to be able to observe any trends in the models. Also, *"The effect of climate change on streamflow and groundwater recharge varies regionally and between scenarios, largely following projected changes in precipitation"* [14]. Varieties in the predicted precipitation will affect the effect on the groundwater. Therefore, it is important, to simulate an ensemble of climate change predictions, which can show the expected spread of the effect climate change will have on the groundwater. Most studies on the effect of climate change on groundwater are carried out on a local plan and show very site-specific results [14]. Therefore, it could be of interest, to create a model which can be used to give reliable estimations of climate change impact on groundwater on a national basis. GEUS, The Geological Survey of Denmark and Greenland, developed a national water resources model (DK-model) which could be used as a tool to assess climate change impacts on the water cycle in Denmark [6]. The DK-model is already in use to model the Danish groundwater and is calibrated for daily use, but it still needs verification in terms of modeling climate change impacts. The danish national water resources model does also struggle to predict the depth to phreatic surface reliable, this is due to the grid resolution as well as the calibration strategy used [25].

The question, that possibly a local model is needed to predict local climate change impacts on groundwater, arises beacause several studies state that local smaller scale models are needed to predict local climate change impacts on groundwater [7] and [18]. This statement though, is mainly based on general guidelines on groundwater modeling which state that a high discretization will result in a more precise model [22], and has not been further investigated in predicting climate change impacts on groundwater. One study shows that the dominating source for uncertainty in predicting groundwater in a future climate comes from natural climate variability and the climate model [19].

They do also state that uncertainties connected to the hydrological model are important [19]. In one case, it is recorded that climate model uncertainties dominate compared to uncertainties in geology when predicting groundwater heads, but that the importance of the geology increases with increasing climate change [23]. Another study showed that the climate model uncertainty was the driving uncertainty when modeling predicting future hydraulic heads [30]. These studies highlight that uncertainties related to the changing climate often out scale the uncertainties arriving from the hydrological models, which gives good reasons to investigate the applicability of larger models for climate predictions on groundwater further. To be able to investigate this further, a highly calibrated hydrological groundwater model is needed to be able to minimize the uncertainties arising from the hydrological model, and focus on the predicted change in groundwater heads in future climate change scenarios.

1.1 Problem Statement

It is known that climate change will affect groundwater recharge rates, and thereby the groundwater aquifers including the groundwater heads and groundwater resources [11]. But it is difficult to give good estimates of the impacts due to the slow response of the groundwater to a changing climate [14]. Also, it is questioned if a nationwide groundwater model can show the regional impacts, or if models on the size of a catchment or a specific site are needed to track those impacts. The Danish and the British geological surveys are investigating on how and in what extent their national groundwater model can be applied for a nationwide risk assessment for the effect of climate change on the groundwater [6] and [13]. This study focuses on the divergence of different-scale models in the case of climate change impacts on groundwater and will finally give an idea of how differently the used models perform. The three different-scale models which are used, are on a national scale, a regional (catchment) and a local scale. The study site, as well as the extent of the local model, is a lake, a town and their surroundings in central Jutland. Both the lake and the town are called Sunds, and have had issues with groundwater flooding during the last years. The other two models are the national groundwater model of Denmark and a model for the catchment of Storå, where Sunds lies within. The main research question in this thesis is:

Is the national model applicable for investigations in smaller regions, or do we need to implement models with higher spatial resolution to be able to asses climate change impacts on the groundwater on a local scale?

To answer the research question, the following sub-goals are formulated:

- Adjust and calibrate three different-scale groundwater models to be used for climate predictions on a national, regional and local scale. The models cover respectively Denmark, the catchment of Storå and Sunds Lake, which has a history with groundwater flooding [25].

The national model has a discretization of 500 x 500 m, the catchment model of the Storå catchment has a discretization of 100 x 100 m and the local model for the area of Sunds has a discretization of 25 x 25 m.

- Determine the changes in the shallow groundwater, based on three different climate scenarios.

  The study focuses on the shallow groundwater, because the area of Sunds is known for its vulnerability to groundwater flooding. To model a wide spread of climatic impacts, three different climate projections are chosen, which illustrate the wide range of the Euro-Cordex climate ensemble.

- Evaluate the differences on the simulated depth to phreatic surface, based on the different models and climate scenarios used, and quantify the differences of the expected flooding in the various scenarios on the area of Sunds Lake.

  To evaluate the differences, the model results will all be compared in the area of Sunds, and will be compared in regard to how they predict groundwater level rise differently, and further quantified in assessing the area flooded during an average winter scenario in the future.

1.2 Background

Studies conducted in the field of the effect of climate change on groundwater are rare and if they are conducted, they are mainly focusing on the groundwater resource on a specific site [26]. Even less research focuses on the impact of climate change on the phreatic surface and groundwater flooding in the future. Only few countries, such as the Netherlands, Denmark and Great Britain have investigated the problems of groundwater flooding as response of climate change, those studies do also mainly focus on a local scale and use very site specific models [15], [21] and [12]. Still, research shows that countries in the northern hemisphere can expect higher precipitation rates in future [10], which thereby can lead to a rise in the groundwater table and cause flooding in areas with a short distance to the phreatic surface. Especially seasons with high precipitation will have a higher risk of groundwater flooding.
Denmark is one of the countries, where most climate change scenarios show an expected increase in precipitation [9] and [17] while the current depth to the phreatic surface lies below 1 m in many areas of the country [5], the current depth to the phreatic surface in Denmark is shown in figure 1.1.

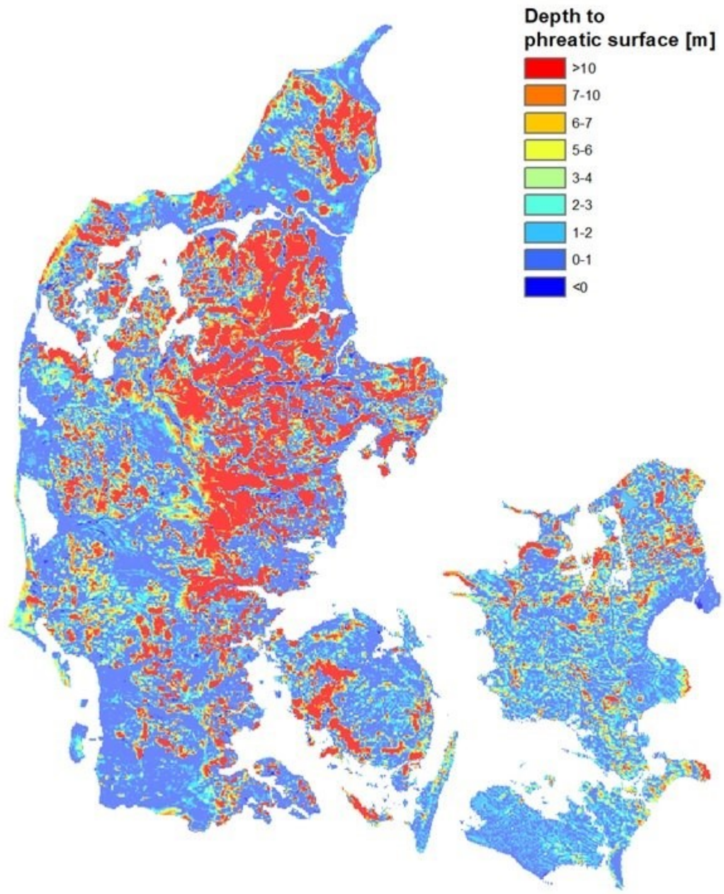

Figure 1.1: Present depth to groundwater table computed with the model from *klimatilpasning* [5].

Based on the shallow depth to the phreatic surface and the increase in precipitation, an increased risk of groundwater flooding can be expected. To decrease socio economic damages caused by flooding, an possible extend of the expected flooding could help

to implement adaption strategies to minimize the damage of groundwater flooding in the future. When looking at figure 1.1 it shows that Denmark has large areas with little depth to the phreatic surface, therefore a nationwide model to predict potential impacts of climate change on the phreatic surface is of interest. GEUS has developed a National Water Resources Model for Denmark (dk-model) which can be used to model the groundwater level in a known time frame [6], but it is yet to be tested if this model can be applied to predict climate change impacts on the phreatic surface. Groundwater responds slowly and has local variations, so a national model would need to have high spatial resolution to predict local changes in the groundwater amplitude [7]. A model with that size (42.700 km^2) would require large computational capacities to model climate scenarios for a prediction. Also, the model would need to run with several climate scenarios, to create a dataset which covers the spread of possible climate change impacts on the shallow groundwater.
Therefore, the idea is, to use the national model to create a nationwide dataset with a change in groundwater level in a 500 m x 500 m grid which then can be added to a local model to give a prediction of the change in that specific location. But it is unknown, if the local variations in groundwater level will stay unchanged in the future, or if these variations also will be affected by changing climatic conditions. To investigate this, the Danish National Water Resources Model has been run with a range of climate scenarios, as well as two smaller models, to evaluate if these three models show the same results for future groundwater levels in a study site. Based on the shallow depth to the phreatic surface and the increase in precipitation, an increased risk of groundwater flooding can be expected. To decrease socio economic damages caused by flooding, an extend of the expected flooding could help to implement adaption strategies to minimize the damage of groundwater flooding in the future.

1.3 Study Site

As study site, the city of Sunds in central Jutland is chosen. The city of Sunds lies in an area with high precipitation and high groundwater levels and has been facing several groundwater floodings [25]. Sunds lake is located north of the city of Sunds. During a project, regarding the renovation of the old sewer system, new geophysical data has been collected to give an insight in the hydrogeological system and is used as basis for the geological model used in this studies local groundwater model. The local model constructed for Sunds covers an area of 47 km^2 and lies within the catchment of the river Storå. Storå flows north of the city and the Sunds lake is part of the river. The area has the highest elevation in the east (60 m) which decreases to around 35 m in the south west. Figure 1.2 is showing the area of Sunds used for the model and where it is located in central Jutland, while figure 1.3 show the terrain in the area.

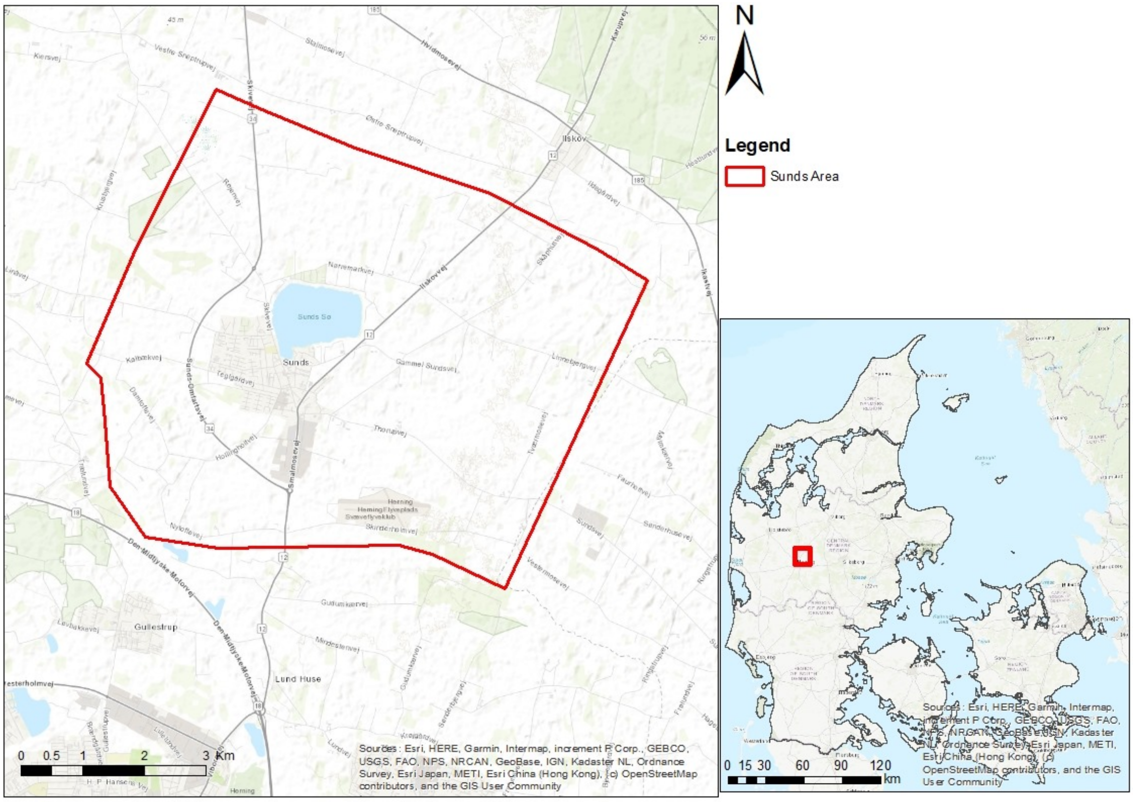

Figure 1.2: The study site location in central Jutland outlined in red.

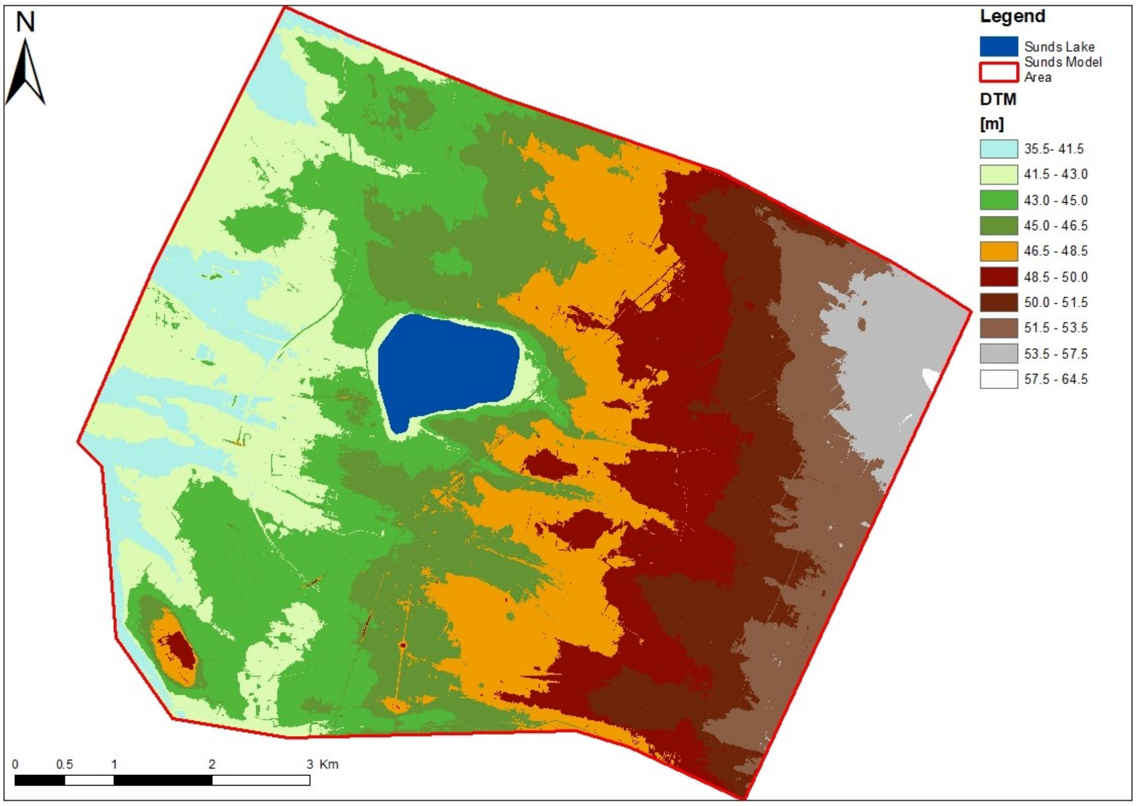

Figure 1.3: The figure shows the terrain in the area of interest, and a decrease in elevation can be seen from the east to the west.

1.3.1 Geology

The geology in the Sunds area is characterized by the Weichselian Ice Age, where Sunds lies in an outwash plain formed by glacial sediments. The geology around Sunds and Sunds lake has been investigated by the HydroGeophysics Group, Aarhus University, GEUS, Herning Municipality, and Central Denmark Region, and is described in two reports, one regarding the geology beneath the lake [27] and one focusing on the area north and southeast of the lake [28].

The geology of the area can be divided into three different origins:

- Post glacial deposits
- Weichselian outwash sediments
- Other glacial deposits

The first five to 20 meters of the landscape is dominated by weichselian sand and gravel deposits, which are followed by layers of different types of clay and sand of varying thickness. From top to bottom, a cross-section can be described as:

- 5 m - 20 m of weichselian sand and gravel deposits
- 2 m - 15 m of Måde group clay
- Around 20 m of mica sand with inclusions of Arnum clay lensen with a thickness of up to 5 m

- 10 m - 25 m of quartz sand
- Around 40 m of Arnum clay

Starting below the lake of Sunds, a north-south oriented buried valley stretches to the southern border of the study site. The buried valley is filled with meltwater sand and gravel, and starts in a depth of 20 m below surface and continues for about 30 m to 40 m in thickness. A cross-section showing the overall geological layers in the area is shown in figure 1.4.

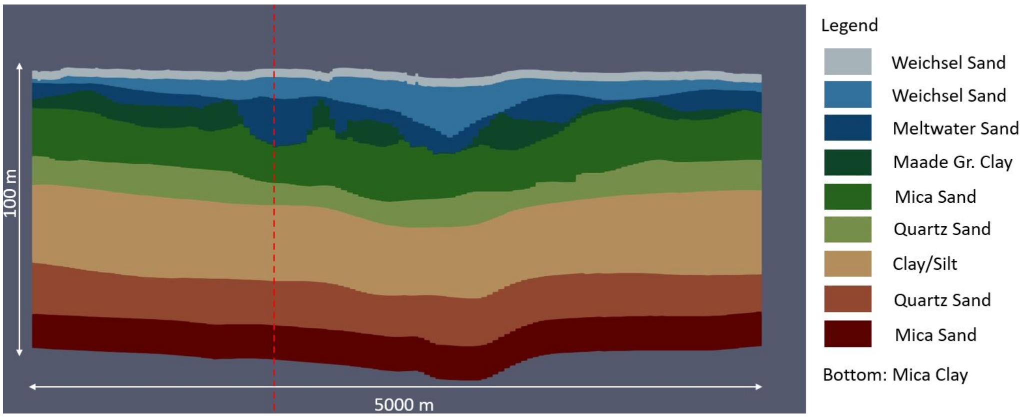

Figure 1.4: The overall geology in the area is shown, the red dashed line indicates the location of the buried valley. The buried valley is the depression filled with meltwater sand.

The aquifers in the area can best be described, as unconfined in the top sand layers, then a noncontinuous layer of clay, followed by semi confined sand layers. Then a thick clay layer creating a fully confined sand layer below. The bottom layer of the geological survey, as well as in the hydrological model is a thick layer of mica clay.

1.4 Future Climate Scenarios

Modeling climate change impacts with numerical models is gaining interest with developing new general circulation models (GCMs) and achieving a wider understanding of the ongoing processes. Genereal circulation models are climate models based on a mathematical model which includes the circulation of either atmosphere or ocean. Also, a combination where climate models are based on both, the circulation of the atmosphere and the ocean exist. The IPCC (Intergovernmental Panel on Climate Change) states that GCMs are the most advanced tools for simulating impacts of the increasing GHC (Greenhouse Gas Concentrations) on the global climate [8]. When combining those global models with nested regional circulation models (RCMs) they can be used to assess the impact of climate change on the environment on a regional basis consistent. For this study, three plausible climate scenarios are chosen to see the possible extent of future groundwater flooding in the area of of Sunds. As climate scenarios, three scenarios from the Euro-CORDEX initative are chosen, all driven by a representative concentration pathway of 8.5, which represents a rising radiative forcing that will reach 8.5 W/m^2 by 2100 relative to preindustrial levels [29]. The climate models are bias corrected and represent a dry, a wet and a medium model to give a wide spread of possible effects on the groundwater level in Sunds. The three models are selected from an ensemble of 22 models, with the criteria of highest, lowest and the median increase in precipitation modeled for Denmark, based on a present period 1981-2010 and the future period 2071-2100. These periods are also afterwards used when determining the change in groundwater head in the future. The precipitation, based on the three climate models, in the Sunds area is shown in figure 1.5. The figure shows that all three models expect a rise in precipitation in the future.

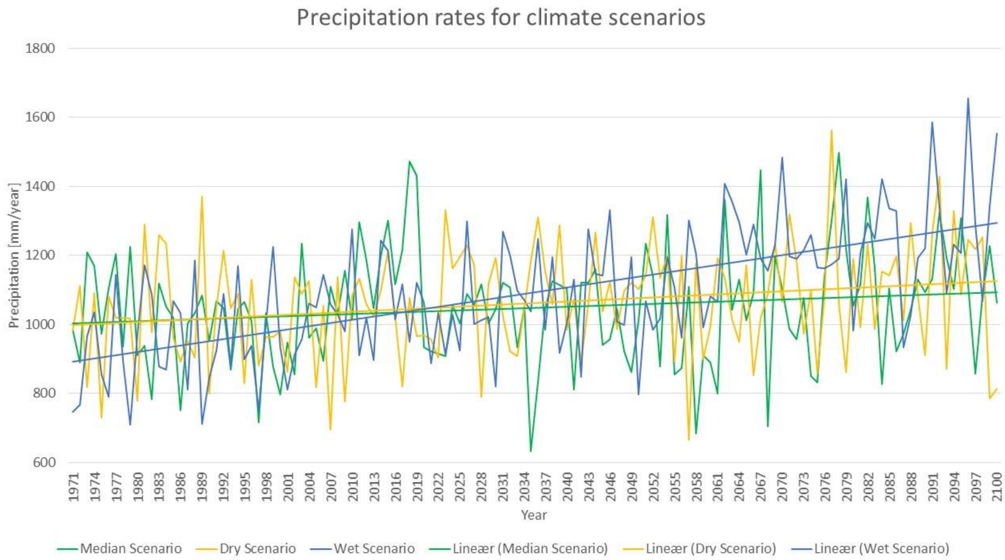

Figure 1.5: Precipitation from the three used climate models for the area of Sunds.The straight lines are the trend lines for each scenario.

Both, change in precipitation and change in temperature are modeled by the climate model, while the potential evapotranspiration is estimated by the Oudin equation, which does only require temperature as input [17]. The Oudin equation is formulated as follows if the temperature T plus 5 is larger than 0 ($T+5>0$) [16]:

$$PET = \frac{0.408 \cdot R_e(T+5)}{100} \tag{1.1}$$

Where T is the mean air temperature in degrees Celsius at 2 m height and R_e is the extraterrestrial solar radiation in MJ m^{-2} d^{-1}. When (T+5) is below 0, potential evapotranspiration equals 0. This method to estimate potential evapotranspiration (PET) seem to reproduce the annual PET accurately [17]. Future temperature and potential evapotranspiration are shown in figures 1.6 and 1.7. Also those figures show a rise in temperatures as well as potential evapotranspiration. The average annual temperatures predicted by the climate model, match the actual observed temperatures in the beginning of the period, 7.7 °C in the period from 1961-1990 [1] and 7.8 °C in 1980.

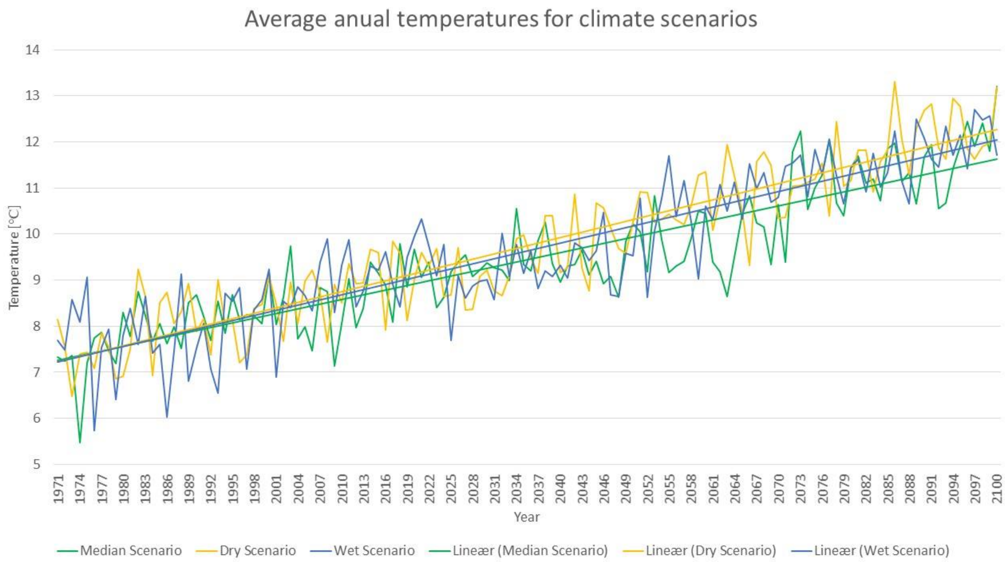

Figure 1.6: Temperature from the three used climate models for the area of Sunds.The straight lines are the trend lines for each scenario.

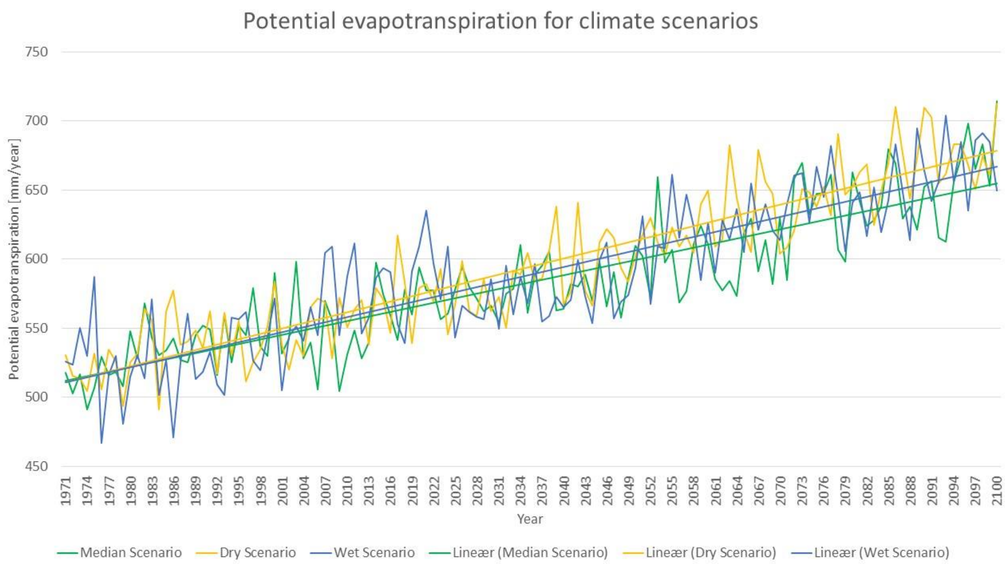

Figure 1.7: Potential evapotranspiration from the three used climate models for the area of Sunds.The straight lines are the trend lines for each scenario.

Chapter 2

Groundwater Modeling

Groundwater modeling is gaining more and more interest throughout recent years [22]. This is due to an increased interest in the groundwater, groundwater resources, groundwater quality and many more [22]. For this project, three groundwater models developed by the Geological Survey of Denmark and Greenland are utilized. All three models needed some adjustments to be feasible for this project, while one of the models still had to be calibrated to secure a qualitatively sufficient model. This chapter will give an introduction to the model code used in the three models, describe the differences between the models, and finally outline the calibration conducted.

2.1 The Models

In this project, three fully integrated groundwater/surface water hydrological Mike She/Mike Hydro models are used. The models include three modules which describe routing and distribution of water in the model area, overland flow, the unsaturated zone, and the saturated zone. The description of the modules is based on the MikeShe user guide V. 1 [2] and the MikeShe reference guide V. 2 [3]. The three modules are described as follows:

- Overland Flow: Overland flow is generated when the ponded water in a surface cell exceeds the detention storage capacities of a surface cell, overland ponded water is caused by more water entering a surface cell, than infiltrated. The surface topography then determines the routing of the water on the surface, while water is infiltrated based on infiltration capacities of the soils. Also, evapotranspiration is included. The equation used to calculate the overland flow Q used in the models is:

$$Q = \frac{K\Delta x}{\Delta x^{\frac{1}{2}}} \tag{2.1}$$

  Where K is the Strickler friction coefficient, x is the length of the cell, h is the depth of the free-flowing water and Z represents the slope in the cell. Ponded drainage is calculated with the following equation:

$$\Delta S = (Q_d r + \sum q)\Delta t \tag{2.2}$$

Where the change in storage, ΔS is calculated by the overland drainage and other inputs and outputs such as precipitation, evapotranspiration and infiltration. The overland drain fraction Q_{dr} is calculated by a leakage coefficient C_{dr} and the change in water level during a time step.

$$Q_d r = \frac{d_0 + d_t}{2} \tag{2.3}$$

- Unsaturated Zone: The unsaturated zone is represented in two layers, with the upper layer being influenced by vegetation and therefore evapotranspiration and the lower layer defining the recharge. The effect of the vegetation is described as:

$$S_{intmax} = C_{int} \cdot LAI \tag{2.4}$$

Where S is the maximum canopy interception controlled by the leaf area index (LAI) and a canopy interception parameter (C_{int}). Flow of water in the unsaturated zone can be divided into three processes: Infiltration from the land surface into the soil, evapotranspiration [ET] from the root zone, and the flow in the soil and the discharge to the groundwater. Evapotranspiration is calculated based on the soil water content, soil characteristics and a crop coefficient, k_c and is described by the following equation:

$$ET_{rate} = ET_{ref} \cdot k_c \tag{2.5}$$

The evapotranspiration decreases thereby the water content in the root zone which creates storage in the unsaturated zone.The water content in the root zone can not drop below the water content at wilting point. This method requires time series data for the reference evapotranspiration, as well as root depth and leaf area index. In this two-layer method, flow dynamics in the unsaturated zone are not included, therefore it is assumed, that the water is directly drained into the saturated zone when the water content in the root zone increase above field capacity.

- Saturated Zone: The saturated zone is descried by a combination of Darcys law, and the equation of continuity. The combined equation is written as:

$$S\frac{\delta h}{\delta t} = \frac{\delta}{\delta x}(K_{xx}\frac{\delta h}{\delta x}) + \frac{\delta}{\delta y}(K_{yy}\frac{\delta h}{\delta y}) + \frac{\delta}{\delta z}(K_{zz}\frac{\delta h}{\delta z}) - Q \tag{2.6}$$

Where K is the hydraulic conductivity in three dimensions, h is the hydraulic and Q are the sources and sinks. Drainage in the saturated zone is incorporated as:

$$q = (h - Z_{dr})C_{dr} \tag{2.7}$$

Where the drain flow q is dependent on the hydraulic head h and a leakage coefficient $C_d r$. The actual change in head is then calculated by all flows in and out of the grid cell:

$$\Delta S = (Q_{dr} + \sum q)\Delta t \tag{2.8}$$

The groundwater exchange between the saturated zone and and the rivers are calculated as:

$$Q = C \cdot \Delta h \tag{2.9}$$

Where Q is the exchange flow, C the conductance and Δh the difference in head between the river and the adjacent saturated zone cell.

These three modules are the same used in the three models of this study. In the following sections, the three model setups are described to give an overview of the differences in those.

2.2 National Water Resources Model for Denmark

The National Water Resources Model for Denmark has a discretization of 500 m x 500 m and covers a total area of 43 000 km^2. Due to computational issues, the model is divided in seven sub models, where only model area five (Central Jutland) is used in this study. The model needs still to be verified as tool to calculate flooding scenarios, for that, it needs further adjustments, calibrations and validation [6]. The model is under continuous improvement and part of several studies [24]. The area of the sub-model can be seen in figure 2.1 and covers 11551 km^2. The hydro geological model is based on the FOHM (Fælles offentlig hydrologisk model), the joint public hydrological model. The hydro stratigraphic model describes the geological units, such as outer and inner boundary conditions [24]. For this project, the most recent model version from 2019 is used, some adaptions had to be made to make it possible to use the model in climate prediction. Adaptions were mainly due to prolonging time series data for extractions, vegetation and other time varying variables.

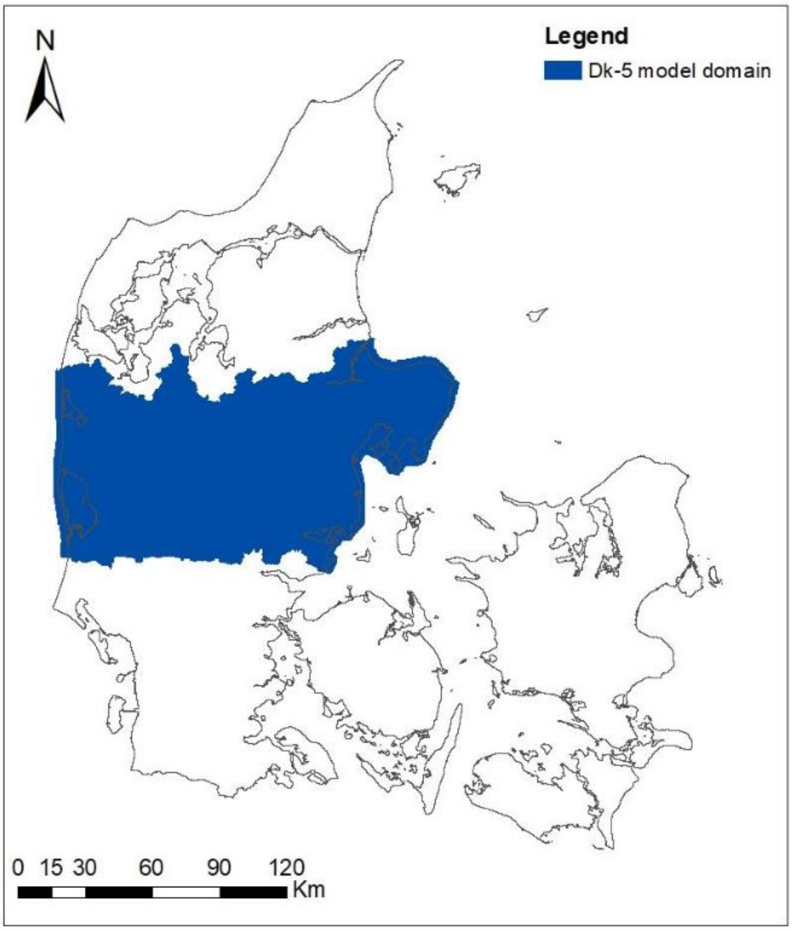

Figure 2.1: The model domain of the National Water Resources Model for the area of central Jutland is highlighted in blue.

The National Water Resources Model for Denmark is mainly calibrated towards the use in larger scale projects and can be used as a screening tool, as hydrological reference, or to investigate larger scale extraction plans on the groundwater resources. In the future, the model may be updated to the use in detail studies on a local scale [24]. Outer boundaries in the DK-model are the coast, the atmosphere and land areas not included in the model domain. The top layer in the model, the atmosphere is a time varying boundary defined by precipitation and potential evapotranspiration data. The boundaries, where the model domain reaches the ocean, a specified head of 0 m is used for the top layer, and no-flow boundaries are specified for other layers. Finally no-flow boundaries are used in the areas where the model domain touches other land areas.

2.3 Storå Model

The Storå Model is a 100 m hydrological model derived from the National Water Resources Model for Denmark. The hydrogeological model in the Storå setup is unchanged because the DK-model already is based on a 100 m grid. The downscaling in the model was done in a project which focused on modeling the surface near groundwater, water level in river and water on terrain in two different study sites in Denmark [25]. Tasks which were conducted throughout the downscaling are [25]:

- Defining the new model domain based on the 100 m digital terrain model from the Danish terrain model *"DHM-Danmarks Højdemodel"*.
- As outer boundary for the Storå Model, the catchment of Storå is used, which gives a closed system without external hydrological input.
- Refining and redefining the rivers and streams in the model domain.
- Re-calibrated against more observations, especially focusing on the phreatic surface.

The recalibration resulted in a significant improvement in the modeled depth to phreatic surface, the modeled results had a mean average area for about 1 m for at least 90 % of the calibration targets [25]. The model domain is shown in figure 2.2.

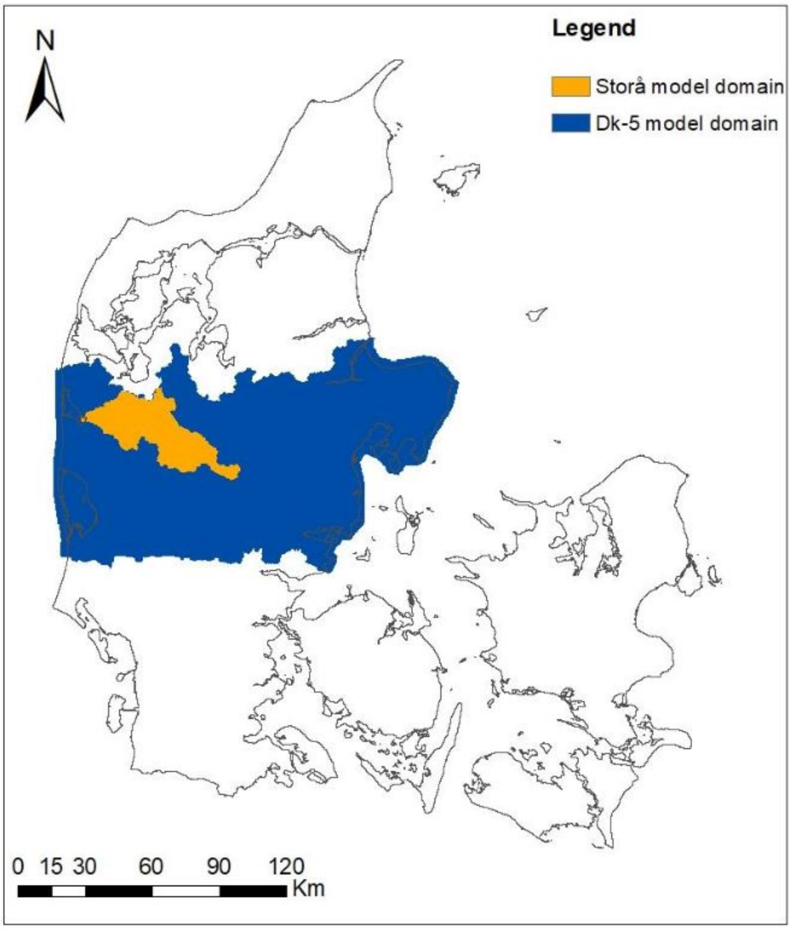

Figure 2.2: The model domain of the National Water Resources Model for the area of central Jutland is highlighted in blue, and the model domain of the Storå model is highlighted in orange.

2.4 Sunds Model

The model for the study site Sunds, has a grid size of 25 m and covers around 47 km^2 and has originally been developed in a project to quantify the effect of renovating a leaking sewer system. The model is based on the Storaa model and results from

Table 2.1: The geological units included in the parameter sensitivity analysis and their initial values, where Hc = Horizontal conductivity, Vc = Vertical conductivity, Sy = Specific yield, and Ss = Specific storage.

Geological unit	Fraction in model %
Late-postglacial deposit (Gyttja)	0.1
Weichselian sandur (ds)	9.0
Meltwater sand (ds)	4.9
Till (ml)	0.3
Meltwater clay (dl)	0.1
Burried valley 1 infill (ds/dg)	1.0
Måde Group clay	2.3
Odderup mica sand	10.4
Arnum clay	27.0
Odderup quartz sand	10.4
Bastrup mica sand	14.4
Bastrup quartz sand	11.2
Klindtinghoved clay	9.0

the Storå model are used as boundary conditions for river discharge, which makes the Sunds model dependent on the model of Storå and lies in the eastern part of the Storå catchment. The model domain of Sunds is highlighted in green in figure 2.5. The geological model used, is an updated model, based on newly obtained geophysical TEM (transient electromagnetic method) measurements which were obtained from GEUS and Aarhus University in another project [28] and [27]. Based on those measurements, a geological 3D voxel model has been created for the Sunds model. The voxel model has a discretization of 25 m x 25 m x 2 and focuses mainly on the upper geological layers. The geology has 16 different geological units which are distributed in 102 layers with a thickness of 2 m following the overall geology of the area shown in figure 1.4. Table 2.1 shows the distribution of the different geologies in the voxel model.

Rivers and lakes are described like in the Storå model, where they were updated. The rivers in the area can be seen in figure 2.3.

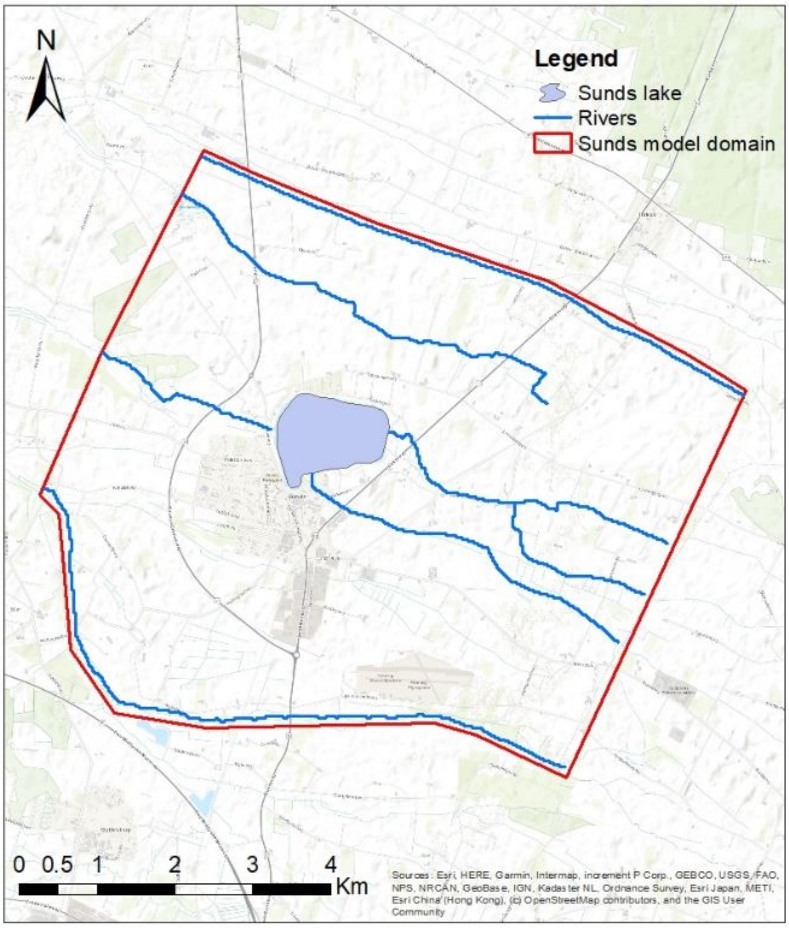

Figure 2.3: Sunds Lake and the rivers included in the model.

For the drainage in the area, three different drain areas are introduced. The three areas are the center of the city with an old sewer system, the outer urban zone with renovated sewers, and the rural areas. The drain depth in the rural area is 1 m below terrain, while the depth to the drain in the sewered area is based on the actual depth of the sewers. A map of the drain areas and drain depths is shown in figure 2.4.

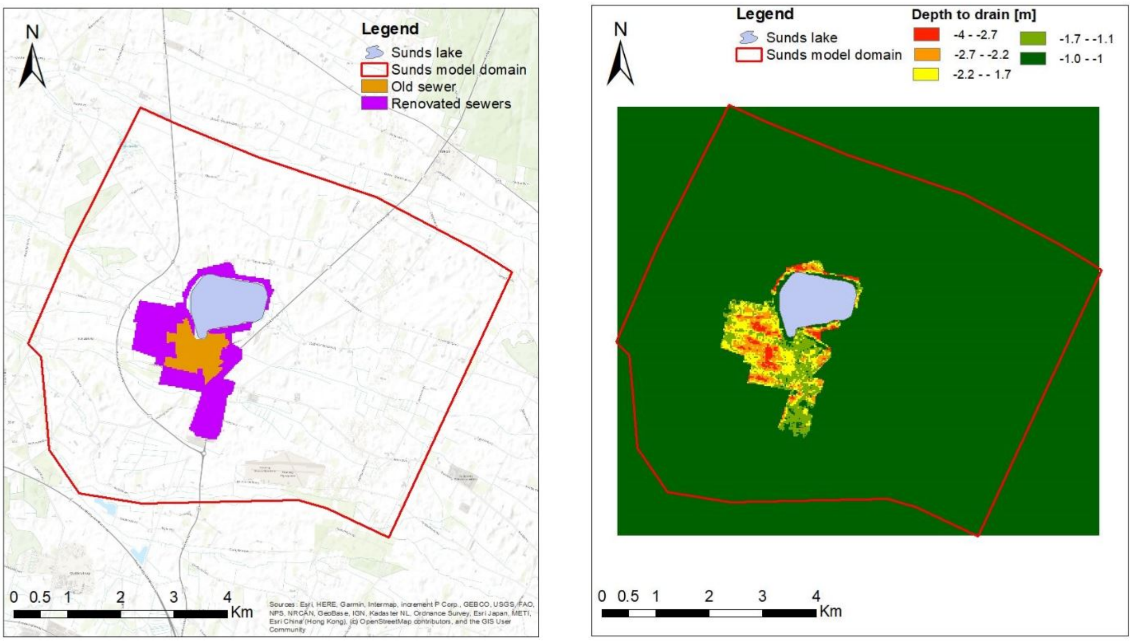

Figure 2.4: The left map shows the renovated sewers (orange) and the old sewers (purple). The right map shows the depth of the actual drain in the model.

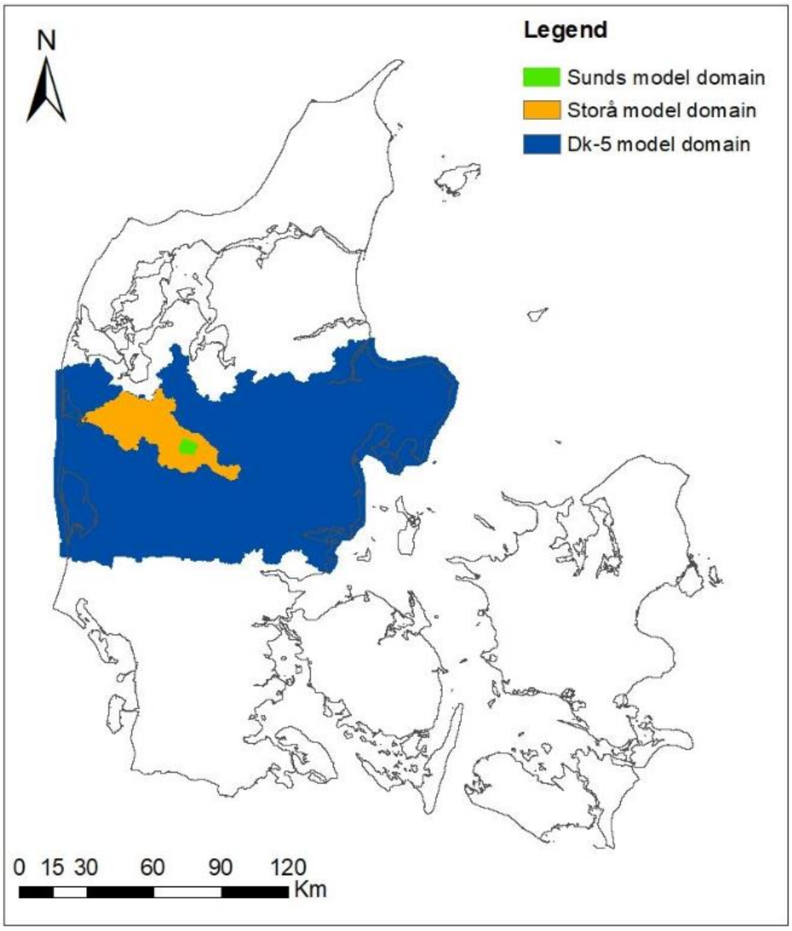

Figure 2.5: The model domain of the National Water Resources Model for the area of central Jutland is highlighted in blue, the model domain of the Storå model is highlighted in orange and the model domain of Sunds is highlighted in green.

The Sunds model is calibrated towards the best possible representation of the groundwater heads in the saturated zone, as well as their amplitude. A detailed description of the model calibration is given in the following sections.

2.5 Sunds Model Calibration

In modeling, calibration is one of the most time demanding and difficult elements [4] and [22], this is due to the many model runs the calibrations needs to perform to be able to identify the sensitivity of the used parameters. In this project an inverse calibration of the model is performed to reach a sufficient optimized model for further simulations. The calibration of the Sunds model is performed with the model independent calibration software PEST, Model-Independent Parameter Estimation and Uncertainty Analysis v. 17, which is the most used software in automatic calibration of hydrological models [4] and [20]. The model is calibrated in the period from 01-01-2010 to 31-12-2020, with an included warm up period from 01-01-2008. The short warm up period is chosen due to computational time, and the dominating sand layers, which gives the assumption that the model is in balance after a short period. Criterions set for the model calibration are:

- The estimated values need to be in a realistic range

- Residuals should be distributed evenly in time and space
- The hydrological characteristics, such as flow directions, groundwater aquifers and flow gradients need to be simulated
- Statistical accuracy on the simulated hydraulic heads, based on the mean error
- Good simulation of the variation in water movements, based on the amplitude error

The criterions are based on GEUS handbook in good use in hydrological modeling [22]. The model is calibrated against groundwater heads of 108 different measuring stations. River discharge is not included, because of unavailability of data, and because the river discharge is highly dependent on the boundary conditions obtained through the Storå model. The sensitivity analysis is carried out on 84 parameters, where the 22 most sensitive parameters were included in the parameter estimation for the model calibration. The calibration improved the model performance to an average error of below 0.3 m on the observed hydraulic heads in the model domain.

The calibration strategy includes many different steps, which are outlined in figure 2.6. During the calibration process, several decisions are made, which all include knowledge on the steps before, like knowing the sensitivity of each parameter, before deciding on which parameters to calibrate. In the next sections, the calibration and calibration results are explained.

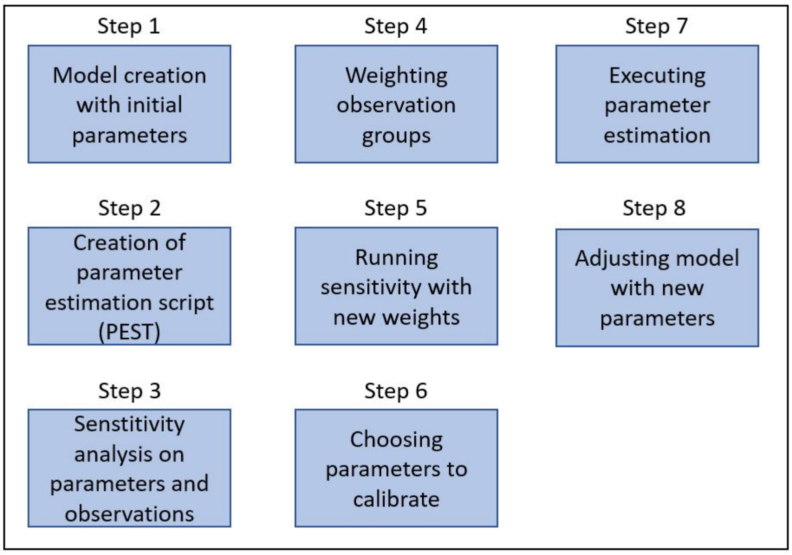

Figure 2.6: Outline of the workflow on calibrating the Sunds model.

2.6 PEST Calibration

The model is calibrated against groundwater heads from 108 measuring stations in the deeper aquifers and in the surface near groundwater. The calibration targets are divided into 3 groups, time series data, single observations, and a synchronized observation round in 2012, the location of these are showed in figure 2.7. The quality of computing the observed heads are calculated in two different ways. Errors for all measurements are calculated as mean error, with the equation:

$$ME = \frac{1}{n}\sum_{i=1}^{n}(H_{obs} - H_{sim}) \tag{2.10}$$

Where H_{obs} is the observed head, H_{sim} is the simulated head an n is the number of observations. Mean error is an expression for how good the model computes the measured heads on average. A positive mean error describes that the simulated hydraulic head, on average, is higher than the observed, while a negative mean error reflects a hydraulic head which on average is simulated lower than the observed. The optimal mean error is 0, which would mean, that the simulated results match the observations. The mean error is a criterion for the average difference between observed and simulated groundwater heads in different areas of the model.

For the time series data, also the error in amplitude is used as calibration target, the error in amplitude is used to see how good the model is in simulating the variations of water movements.

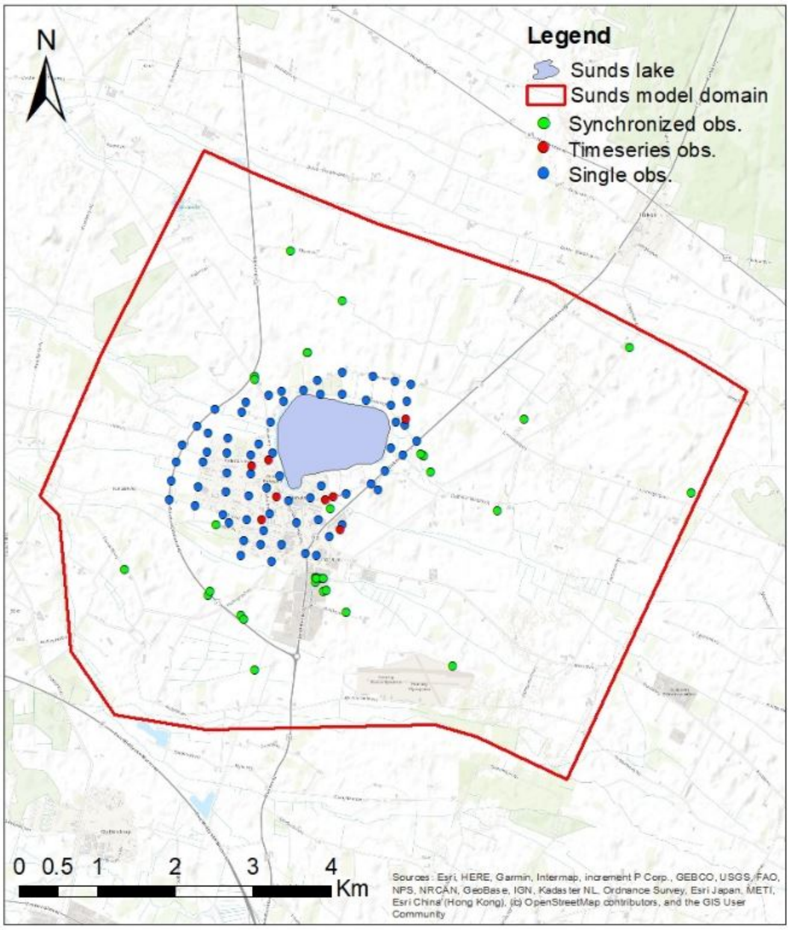

Figure 2.7: The location of the groundwater head observations used for the calibration. (There is an error in the legend, the blue points are the synchronous observation and the green dots are single observations.)

The calibration performed by PEST is done by solving an objective function which is defined as a target for the calibration. The objective function used in PEST is defined as reducing the residuals by changing model parameters, this function is defined as [4]:

Table 2.2: The geological units included in the parameter sensitivity analysis and their initial values, where Hc = Horizontal conductivity, Vc = Vertical conductivity, Sy = Specific yield, and Ss = Specific storage.

Geological unit	Hc [m/s]	Vc [m/s]	Sy	Ss m^{-1}
Late-postglacial deposit (Gyttja)	5.18E-06	5.18E-07	2.00E-01	1.00E-04
Weichselian sandur (ds)	1.00E-04	1.00E-05	3.00E-01	1.00E-04
Weichselian sandur (dg)	1.00E-04	1.00E-05	3.00E-01	1.00E-04
Meltwater sand (ds)	5.00E-05	5.00E-06	3.00E-01	1.00E-04
Till (ml)	6.22E-06	6.22E-07	5.00E-02	1.00E-04
Meltwater clay (dl)	6.22E-07	6.22E-08	5.00E-02	1.00E-04
Meltwater gravel (dg)	1.00E-04	1.00E-05	3.00E-01	1.00E-04
Burried valley 1 infill (ds/dg)	1.00E-04	1.00E-05	3.00E-01	1.00E-04
Burried valley 2 infill (ds/dg)	1.00E-04	1.00E-05	3.00E-01	1.00E-04
Måde Group clay	2.80E-07	2.80E-08	5.00E-02	1.00E-04
Odderup mica sand	2.02E-04	2.02E-05	3.00E-01	1.00E-04
Arnum clay	2.80E-07	2.80E-08	5.00E-02	1.00E-04
Odderup quartz sand	4.62E-05	4.62E-06	3.00E-01	1.00E-04
Bastrup mica sand	4.04E-04	4.04E-04	3.00E-01	1.00E-04
Bastrup quartz sand	4.64E-05	4.62E-05	3.00E-01	1.00E-04
Klindtinghoved clay	1.00E-10	1.00E-10	5.00E-02	1.00E-04
Billund sand	1.00E-04	1.00E-05	3.00E-01	1.00E-04
Vejle Fjord	1.00E-04	1.00E-05	3.00E-01	1.00E-04
Rearranged miocene sand	1.00E-04	1.00E-05	3.00E-01	1.00E-04

$$G(b) = \sum_{i=1}^{n} w_i \cdot r_i^2 \tag{2.11}$$

Where G is the objective function, b the vector with the parameters to be calibrated, r the residual and w the weight given for that residual. The residuals are calculated by:

$$residuals = (H_{sim} - H_{obs}) \tag{2.12}$$

2.7 Sensitivity Analysis

To reduce the number of parameters to calibrate, a sensitivity analysis has been performed prior the calibration. 82 parameters were tested for their sensitivity in the sensitivity analysis, 76 of those parameters are connected to the 19 different geological units, represented as the vertical and horizontal conductivity of the geological layers, as well as specific yield and specific storage. One parameter represents the leakage coefficient of the lake of Sunds, as well as one representing the leakage coefficient of the river up- and downstream of the lake. Two parameters for the rate of inflow and outflow to the overland drainage storage. The last two parameters tested for sensitivity are the time constant for drain, and paved area runoff coefficient. The parameters used for sensitivity estimations are displayed in table 2.2 and 2.3.

The aim of the sensitivity analysis is to show how the different parameters affect the simulated hydraulic heads in the observation location. For the sensitivity analysis, PEST was set up to run the model 82 times with changing one parameter per model run,

Table 2.3: The time constant parameters included in the sensitivity analysis with their initial condition.

Parameter	Initial condition
Leakage coefficient Sunds Lake	1.00E-06 s^{-1}
Leakage coefficient Moellebaek Å	2.41E-05 s^{-1}
Overland ds in	1.00E-03 s^{-1}
Overland ds out	1.00E-03 s^{-1}
Paved area runoff	1.00E+00 s^{-1}
Drain time constant	1.26E-07 s^{-1}

while leaving the other parameters at their base. Some of the geological units are only represented in less than 1 % of the geological cells, and a sensitivity calculated much lower than all the other, so they are excluded in the following tables and graphs. A full list of the sensitivities can be seen in Apendix 1. For the selection of parameters for the parameter estimation, the relative sensitivities are calculated by dividing the sensitivity for that given parameter by the highest computed sensitivity in the set of parameters. This makes it easier to use the sensitivity as a measure to choose parameters used for the calibration.

$$Sens_{rel} = \frac{Sens_i}{Sens_{max}} \tag{2.13}$$

The calculated relative sensitivities can be seen in figure 2.8, based on that, a total of 13 parameters were chosen to be directly included in the sensitivity analysis. Parameters were chosen based on their sensitivity, their geological distribution, and based on having all parameter groups represented in the calibration.To be able to calibrate on even more parameters, some parameters related to the ones directly included in the calibration, are tied to the parameters included in the calibration. Tying a parameter means, that the parameter is changed by the same fraction as the parameter it is tied to. For example: The vertical conductivity of a clay unit is tied to the horizontal conductivity of that same clay, when the horizontal conductivity now is adjusted to improve the model, the vertical conductivity is adjusted as well with the same fraction. Table 2.4 shows the parameters tied to another parameter in the calibration, as well as which parameter they are tied to.

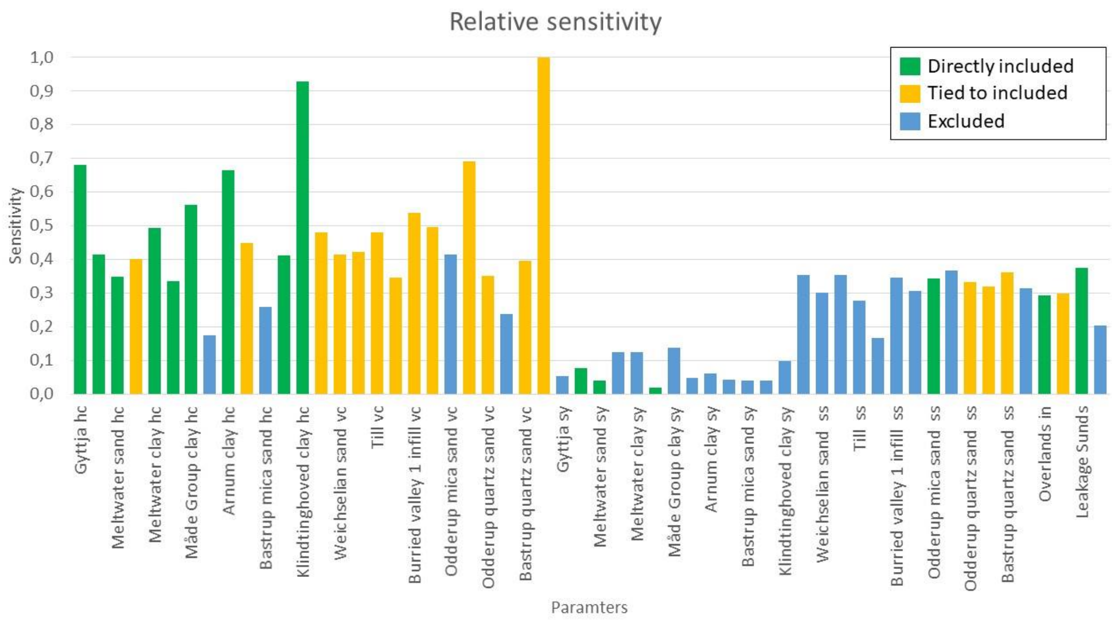

Figure 2.8: The calculated relative sensitivities for the parameters included in the sensitivity analysis. The Green bars show the parameters directly included in the parameter estimation, the yellow bars are parameters linked to the included parameters, while the blue parameters are excluded of the calibration. When parameters are linked, it means that these parameters are adjusted together with the included parameter during the parameter estimation.

Table 2.4: The parameters included in the calibration, and the parameters which are tied to them. Ba. stands for Bastrup, Mw. for meltwater and Od. for Odderup.

Directly included	Tied 1	Tied 2	Tied 3
Gyttja hc	Gyttja vc		
Weichselian sand hc	Weichselian sand vc		
Mw. sand hc	Mw. sand vc		
Burried valley hc	Burried valley vc		
Ba. quartz hc	Ba. quartz vc	Od. quartz hc	Od. quartz vc
Mw. clay hc	Mw. clay vc	Claey Till hc	Claey Till vc
Måde Group clay hc	Måde Group clay vc		
Arnum clay hc	Arnum clay vc		
Klindtinghoved clay hc	Klindtinghoved clay vc		
Weichselian sand sy	Meltwater sand sy	Burried valley sy	
Od. mica ss	Od. quartz ss	Ba. mica ss	Ba. quartz ss
Leakage coefficient Sunds Lake			
Overland ds in	Overland ds out		

Also the sensitivity of the calibration targets is tested, to see if and how much they are affected by changing one of the parameters. That analysis showed that all calibration targets were sensitive to changes in the parameter values. Based on those sensitivities and an evaluation of the observation groups, weights were given to the observation groups for solving the objective function minimizing the error computed by the model. The sensitivities for the calibration targets can be seen in appendix A.

2.8 Calibration of the Sunds Model

For the calibration of the model, weights were given to the four observation groups. The weights are based on the sensitivity of each group, their initial error, their distribution in time and space and an evaluation on how trustworthy their observations are. Normally, the weighting would also include the type of data, but in this calibration, only hydraulic head is used as calibration targets. The weights given each observation are displayed in table 2.5 and are distributed, so a total weight of 100 % is reached.

Table 2.5: The weights given for each observation group during the calibration.

Observation group	Weighting [%]
Time series mean error	35
Time series amplitude error	30
Synchronous measurements mean error	20
Single observations mean error	15

The time series mean error and error in amplitude on the time series are weighted the highest because they consist of hourly measurements throughout the calibration period. The mean error is weighted higher than the error in amplitude, because it is found more important to predict the actual hydraulic head than the variations in the amplitude. The synchronous measurements are weighted 20 % because they give a good snapshot of the hydraulic head at a specific time over a larger area. The single observations are weighted the least, because they are only single measurements with little information, so there could be some errors connected to those. They are still included in the calibration to give a better spatial distribution of observations in the area, because the time series observations, as well as the synchronous measurements are mainly located around the lake.

Calibrating the model is an iterative process where the objective function is solved to decrease the residuals as best as possible. The residuals are minimized by finding the combination of parameters which reduce the objective function the most. PEST uses a gradient based method to solve the objective function described in equation 2.11. The gradient based method is outlined in figure 2.9.

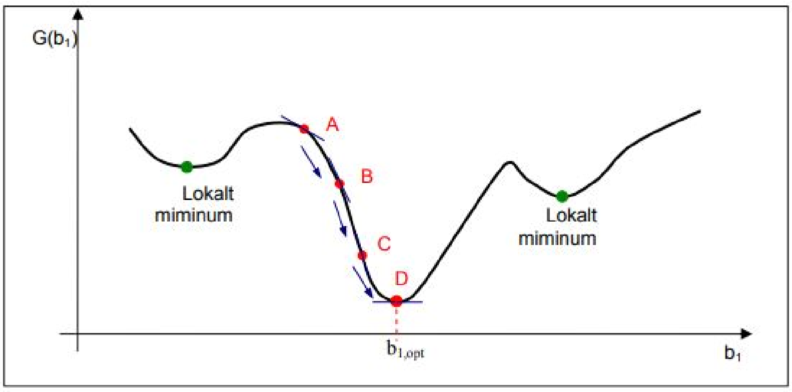

Figure 2.9: Illustration of the gradient based method from [22].

In the gradient based method, the calibration starts at a random point of the line in figure 2.9 based on the initial parameters in the parameter vector. Based on that, the slope of the curve in that point is calculated, which gives information about in what direction the parameters need to be adjusted. After adjusting the parameters, a new location and slope is found. This process is repeated until the slope is as close as possible to zero. A visualisation of the iterative process is shown in figure 2.10.

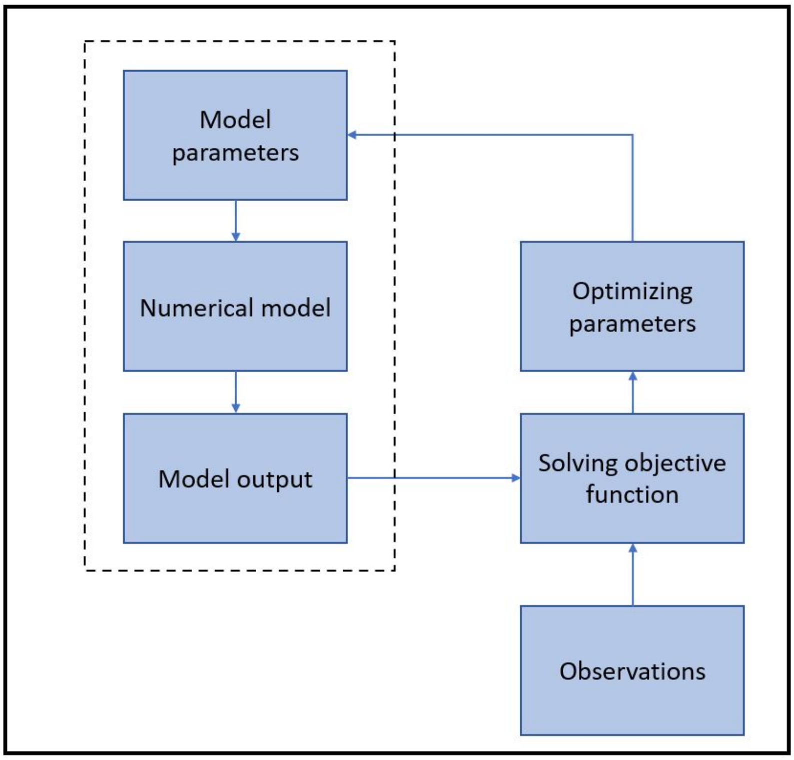

Figure 2.10: Visual overview of the automated calibration, the steps in the dashed line are linked to running the hydrological model, while the steps outside are performed on the model results to estimate new parameters for the next iteration.

The calibration stopped after three optimisation iteraions and a total of 50 model runs and resulted in an adjustment of all included parameters. The calibration decreased the objective function by around 30 %, mainly on the error of the time series mean error (13 %) and the time series amplitude error (13 %) The mean error on the single observations was reduced by 3 %, while no improvement was achieved in the synchronous measurements mean error. The mean error after the calibration can be seen in figure 2.11. The full calibration log is in appendix B. The parameter changed the most, was the horizontal conductivity from the weichselian sand, all estimated parameters are shown in appendix B.

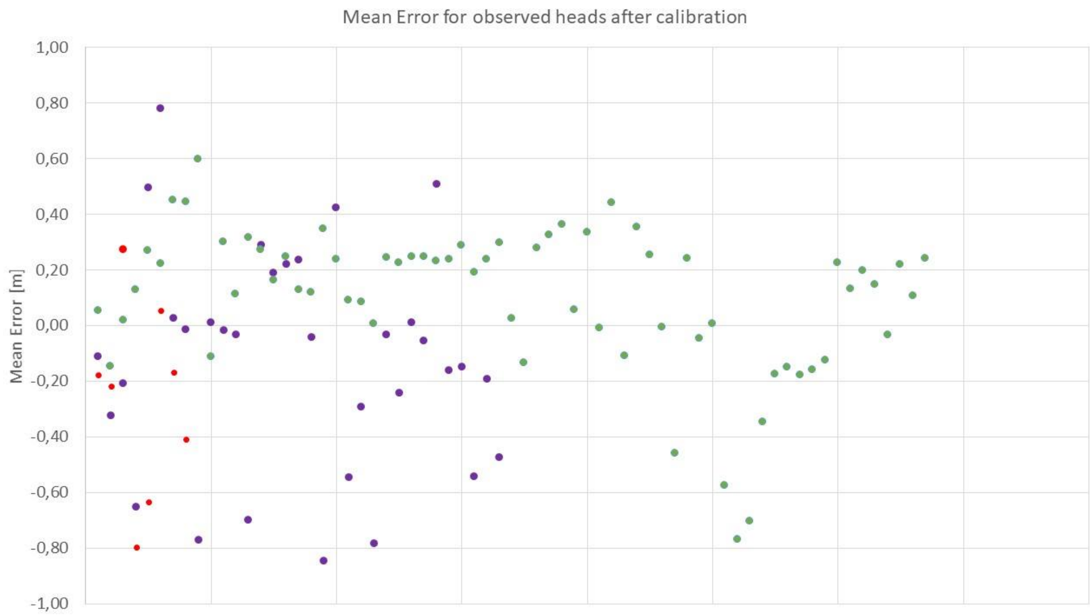

Figure 2.11: The mean error for the measurements after the finished calibration. Red points = Time series data, green points = synchronous observations and purple points = single observations.

The calibrated model is validated against the same time series observations as used for the calibration, just in the period from 01.01.2008-31.12.2009 where the average mean error was computed to 0.24 m. The model was afterwards used as the new updated Sunds model in this project.

Chapter 3

Results and Discussion

The results chapter in this report is divided in two sections, one focusing on the scaling difference between the models and the impact of that on the predicted future change in groundwater level based on three different climate scenarios. The second section is focusing on how the different climate scenarios together with the three models are predicting groundwater flooding in the area of Sunds.

3.1 Scaling Differences

As mentioned in the introduction, groundwater models with high discretisation are preferred when modeling local groundwater problems, but it is also unknown how important the model discretisation is compared to for example climate variables in predicting climate change impacts on the groundwater. To investigate this, three models with different discretisations are run to predict the change in groundwater level in a future scenario. The future scenario is evaluated on the difference in groundwater table from a present period, 1981–2010 and a future period 2071-2100. The median rise in groundwater table for the wet climate scenario is shown in figure 3.1 and 3.2, the maps show an average rise in all of the three used models, where the Storå model stands out by having several areas with a decrease in groundwater table (figure 3.1 right map), those are though in the range of few millimeters to a maximum of 5 centimeters. Another thing which catches the eye, is that the Sunds model (figure 3.2) seem to catch more local variations, and also, to estimate a greater change in groundwater level compared to the other two models. To investigate the difference between the calculated changes, the Storaa and DK-model results are downscaled to 25 m x 25 m and then, the numerical difference between the results is computed, shown in figure 3.3 and 3.4. The different in the results is showing the same picture which already could be guessed from looking at the change in groundwater table for this scenario. The Storaa and the Dk-model seem to produce results similar to each other, while the results from the Sunds model show some larger variations especially in the east of the area. But is this difference mainly due to the difference in grid size and thereby more detailed distribution of the change in groundwater head, or does it arise from other updated and recalibrated parameters in the model area? To investigate the importance of the grid size, the Sunds model results are re-scaled to a 500 m x 500 m grid by using the nearest neighbor interpolation. Also the Dk-model results are downscaled using a bilinear interpolation, which smoothes out the data and maybe distribute the change of the groundwater table differently between the cells the results for both approaches are shown in figure 3.5. Rescaling does not seem to change the outcome of the difference which indicates that the other changes in the model description in the Sunds model are the driving forces in the distinctions between the results of the three models.

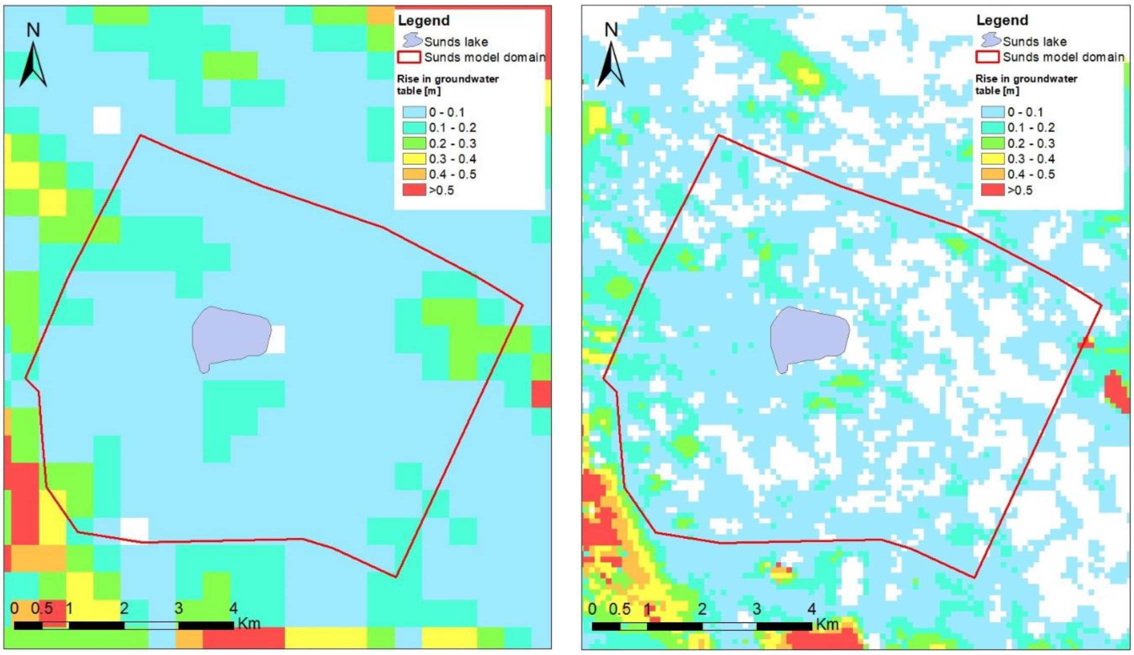

Figure 3.1: The left map shows the median rise in groundwater table computed by the Dk-model for a future wet climate scenario. The right map shows the median rise in groundwater table computed by the Storå model for a future wet climate scenario. The white areas are, where a decrease in groundwater is predicted.

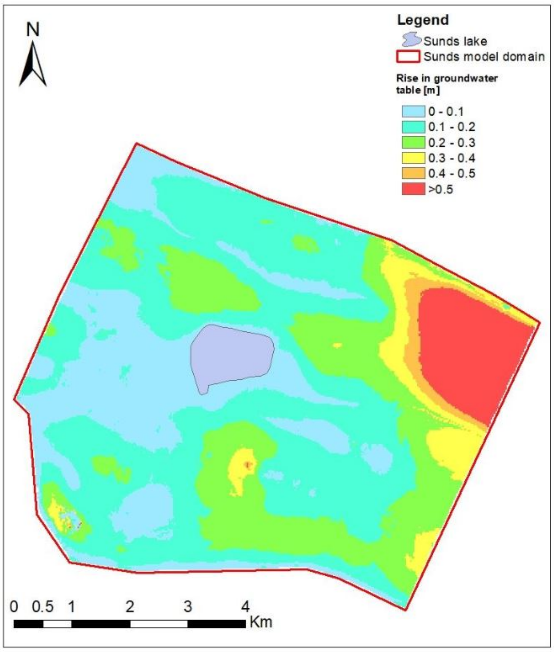

Figure 3.2: The median rise in groundwater level computed by the calibrated Sunds model in a wet climate scenario.

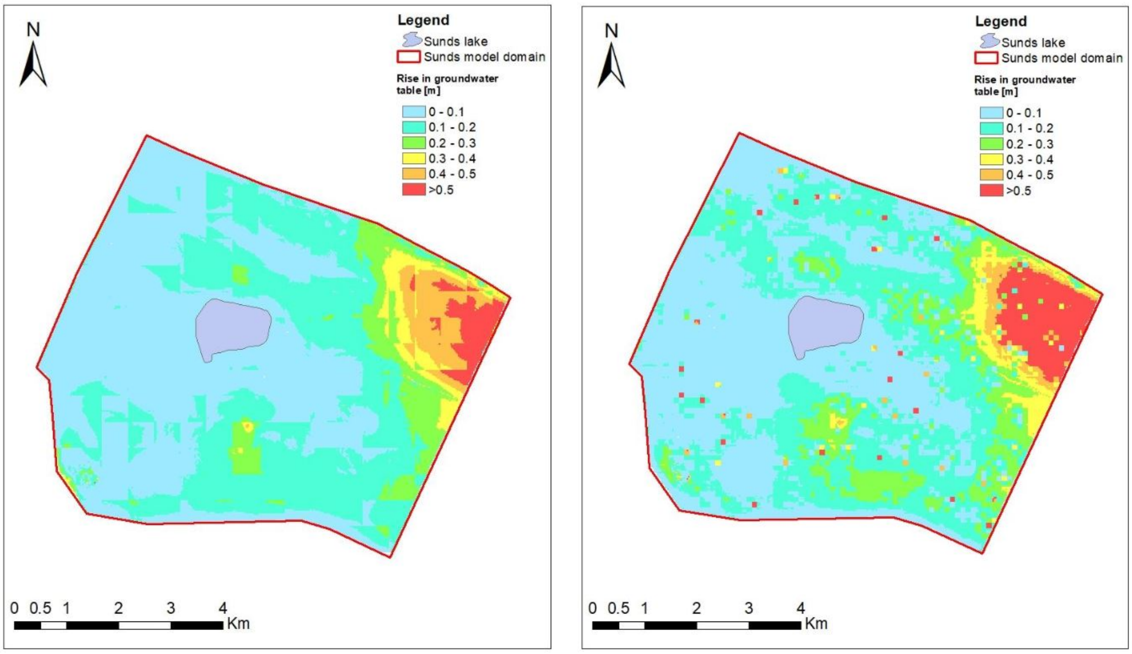

Figure 3.3: The left map shows the difference in the results for the median rise in groundwater between the Sunds and the Dk-model during a wet climate scenario, while the right map is showing the difference between the Sunds and the Storå model in the same scenario.

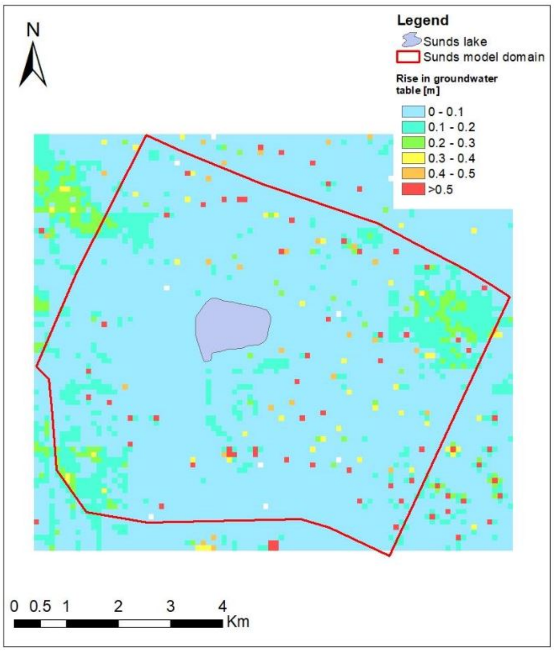

Figure 3.4: The difference in the results for the median rise in groundwater between the Storå and the Dk-model during a wet climate scenario.

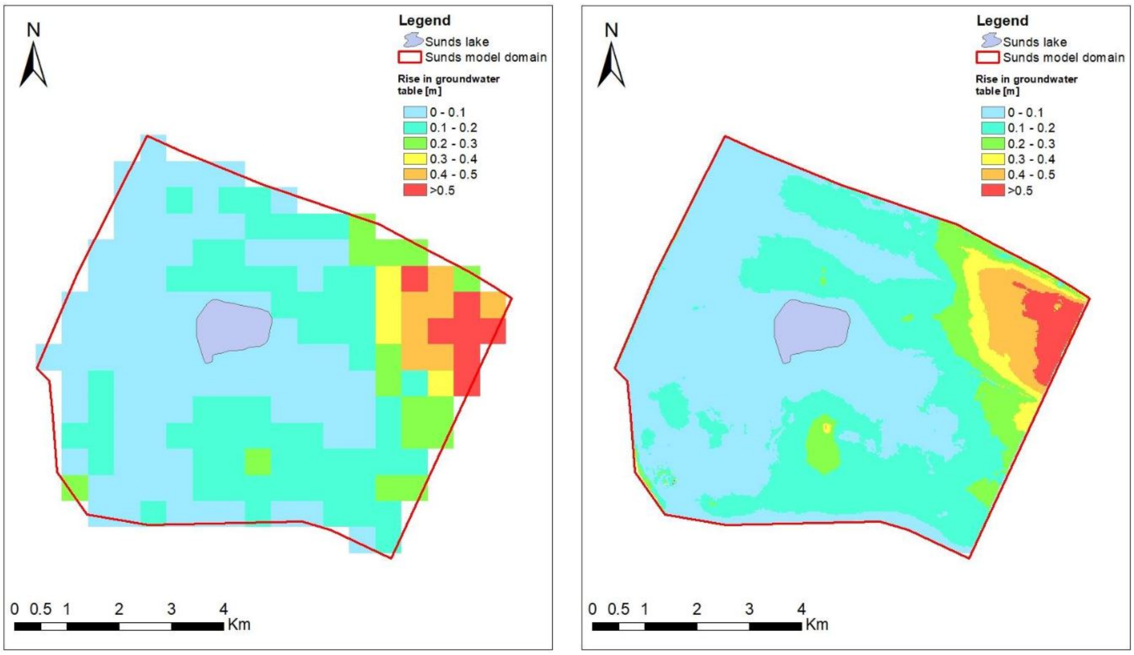

Figure 3.5: Both maps show the difference in simulated change in groundwater level between the Dk-model and the Sunds model. The left map shows an upscaling of the Sunds model results using nearest neighbor, while the right map is showing a downscaling of the Dk-model results using a bilinear interpolation.

The analysis above shows that the Sunds model is simulating bigger changes in the shallow groundwater than the two other models are, it is hard to distinguish the actual difference between the results predicted by the Storå and the Dk-model. The results above are all based on the medium change in the shallow groundwater, but how do the models perform in simulation peak values in an extreme situation? To check that, the difference in the 99 percentile in the results for the wet climate scenario is calculated based on the winter periods in 1981-2010 and 2071-2100. A winter period is defined as first of december to 28th of february and chosen, because these periods are expected to give the highest groundwater tables. The results for the difference between the 99 percentiles in winter between the present period 1981-2010 and the future period 2071-2100 are shown in figure 3.6 and 3.7. It seems like the Storå model is catching many of the same changes the Sunds model is simulating, but the Sunds model results are marginal larger than the ones predicted by the Storå model. Those results are indicating a better modeling of local variations by the model with the most detailed discretisation. For the three models and the two scenarios (Dk-model, Storå model, Sunds model, median change in a wet climate scenario and the 99 percentile of the winter change in a wet climate scenario) the average rise in groundwater level is calculated for the area of Sunds (3.1. Those results show a much larger average rise in groundwater table for the Sunds model compared to the two other models, both in a median and an peak situation. Also these results indicate that the adjustments done to the Sunds model change the simulation results of climate change impact predictions significantly. But where does these differences arise? To analyse what areas of the model are impacted the most and what dynamics cause the different simulations, water balances are calculated for the three models for the wet climate scenario. The water balances are calculated for the whole simulation period (1971-2100) but are focusing on the area north of the lake, where an increase in groundwater level is predicted. The area for the water balance is outlined in figure 3.8. The water balance (3.2) shows that there is faster or at least more flow in the saturated zone for the Dk-model and the Storå model compared to the Sunds model. This could indicate that the updated geology in the Sunds model affects the subsurface flow dynamics significantly. Chart plots of the water balance for the models are shown in appendix C. In the next section, the possibility of climate change induced groundwater flooding in the area of Sunds will be evaluated.

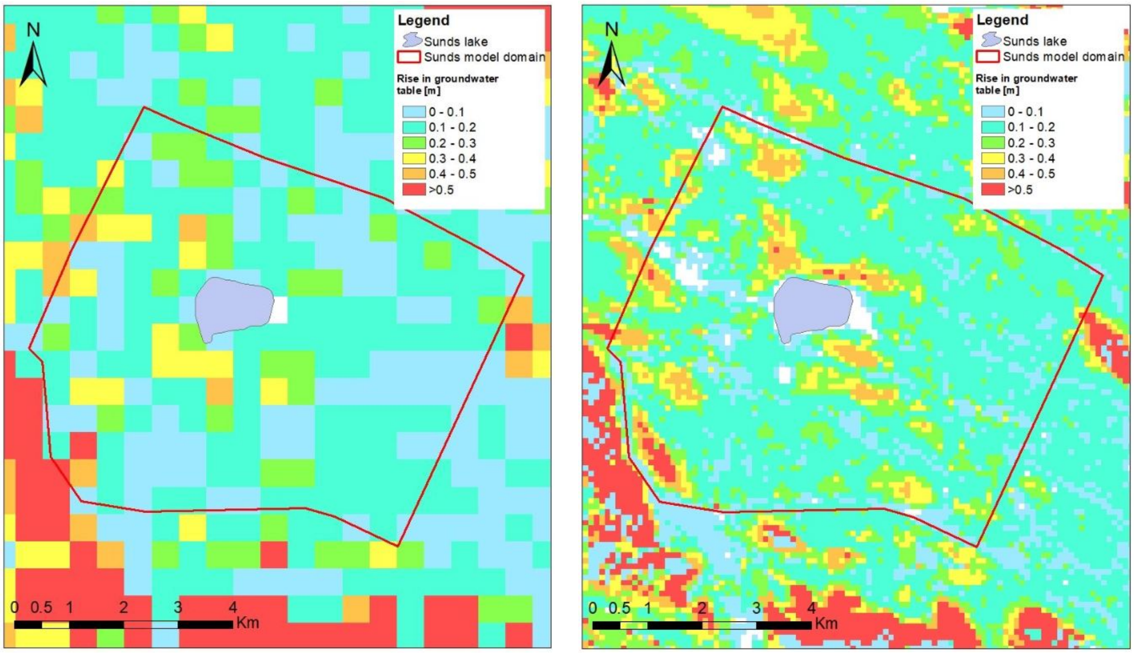

Figure 3.6: The left map shows the 99 percentile rise in groundwater table computed by the Dk-model for the winters in a future wet climate scenario. The right map shows the rise in groundwater table computed by the Storå model for a future wet climate scenario.

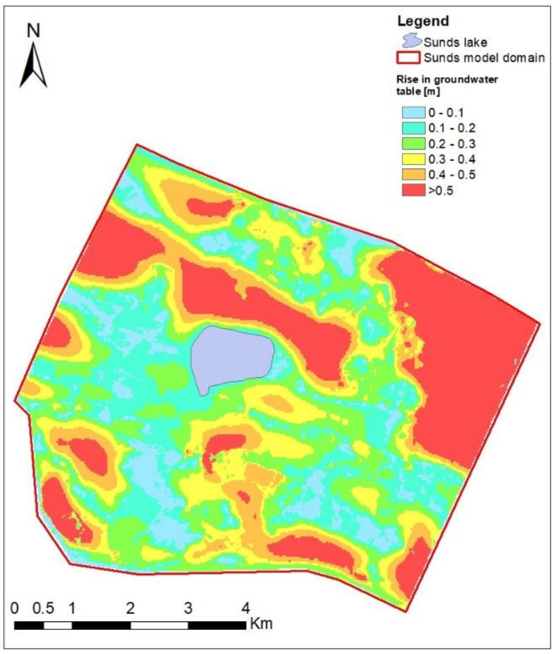

Figure 3.7: The change in groundwater level computed by the calibrated Sunds model.

Table 3.1: Average rise in groundwater table in the present and future period (1981-2010 and 2071-2100) for the three models used. The average is calculated on a grid cell basis for the model area of Sunds

	Dk-model	Storå model	Sunds model
Wet climate scenario median change	9 cm	2 cm	20 cm
Wet climate scenario 99 percentile	17 cm	19 cm	36 cm

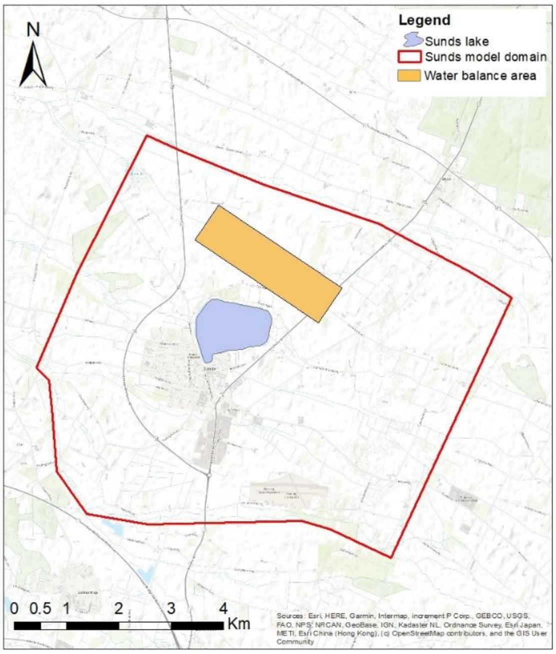

Figure 3.8: The area used to calculate the total water balance for all three models for the whole modeling period (1971-2100) is highlighted in orange.

Table 3.2: The calculated total water balance for the whole modeled period (1971-2100) for the three models in a wet climate scenario. All values are in mm. UZ stands for unsaturated zone, SZ for saturated zone and OL for overland.

Water balance parameter	Dk-model	Storå model	Sunds model
Precipitation	144331	139169	142743
Evapotranspiration	67119	79582	73946
UZ boundary in	-	556	435
UZ boundary out	-	286	330
SZ boundary in	222658	200323	162929
SZ boundary out	230952	206462	134053
UZ storage change	10	-9	-4
SZ storage change	97	-159	-124
OL storage change	0	0	-2
OL to river	-	2262	6334
SZ to river	66202	54270	33017
River to SZ	0	1	71
SZ to external river	-	1197	924
UZ to SZ	84947	109771	68679
SZ to UZ (incl. Evaporation)	448	250	4920
Irrigation	7294	51917	1148
Pumping	-6926	-46212	-1137
Error	23	137	38

3.2 Climate change induced groundwater flooding

Predicting the change in groundwater table for the wet climate scenario showed that all three models predict a rise in groundwater, both for the median of the simulated results, but especially for a critical scenario, calculated as the 99 percentile of the simulated groundwater level in winter. These results make it interesting to investigate if this rise in the shallow groundwater head can result in future groundwater flooding, and in what extent do different models and different scenarios predict those flooding.
After computing the three climate scenarios for the three different models, the results are compared with focusing on the model area of Sunds, and the depth to phreatic surface, to see how differently the models perform when investigating flood risks. The results are evaluated based on the difference between the simulated hydraulic heads in the Sund model area, simulated using different climate models, and a present assumption of the spatial distribution of the groundwater based on the calibrated Sunds model. The Sunds model is used to predict the spatial distribution of the groundwater in the Area.
In figure 3.9 the areas of the model area, with a depth less than 0.5 m to the phreatic surface and the are witth a depth of 0.5 m - 2 m are shown. The depth is calculated as the average depth to groundwater for the simulated winters and for the simulated summers in the period from 2008 - 2020, based on climate observations as input. These two periods are selected to represent a normal winter and summer situation because those seasons are expected to be the minima and maxima of the groundwater table.

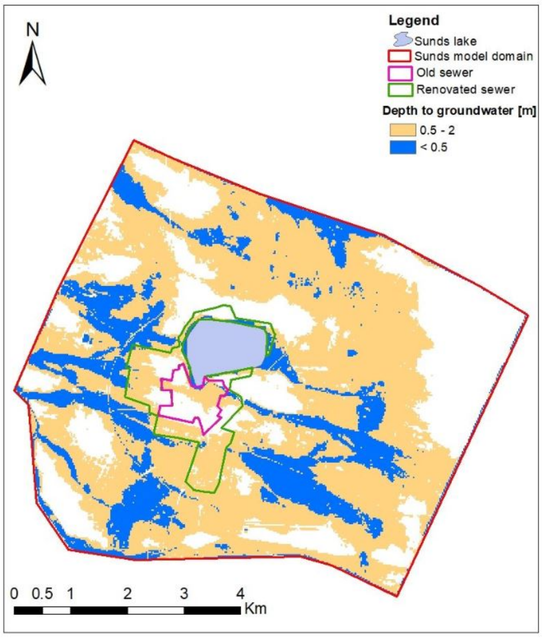

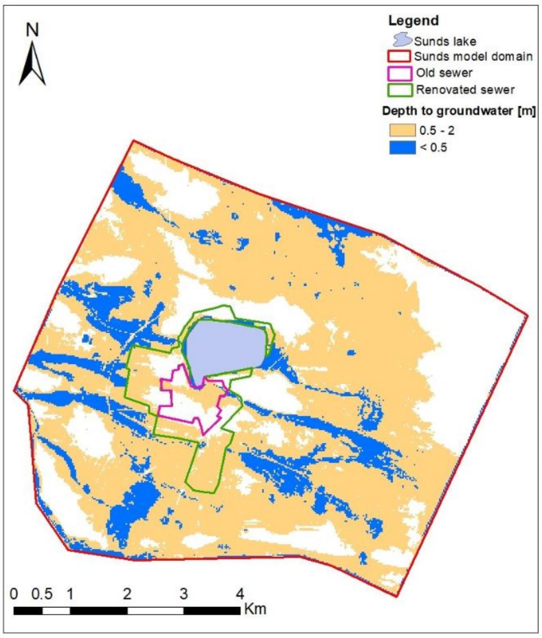

Figure 3.9: Blue areas have a depth to phreatic surface of less than 0.5 m while orange areas have a depth between 0.5 m and 2 m. On the left side an average winter situation, right side an average summer situation. Simulated with the Sunds model.

Figure 3.9 shows that the winter scenario has larger areas with high standing groundwater, which in the following will be used as the average risk situation for flooding in the future. Also a depth of less than 2 m in the urban areas will be considered a risk scenario in the case of basement and other infrastructure flooding. Here only areas within the sewer system are taken into consideration when estimating basement/underground infrastructure flooding. During a present winter simulated with the Sunds model, as shown in figure 3.9, the area does already struggle with groundwater on terrain, as well as groundwater levels inside the city considered a risk for basements and other underground infrastructure. Simulated groundwater levels show that 2.91 km^2 of the area have water on the terrain during the winter, as well as 0.09 km^2 of the sewered area show water on terrain. And about 1.9 km^2 of the sewered area has a depth below 2 m to the groundwater table. The modeled area of Sunds is 47 km^2 and the sewered area stretches for about 3.2 km^2. The 99 percentile change in groundwater, simulated by the three models, is added to the present depth to groundwater, to create a critical future risk scenario in terms of groundwater flooding. The results are shown in figure 3.10 and 3.11. Based on the figures (3.10 and 3.11) it is hard to see any differences in the results, therefore the affected areas for each category (groundwater on terrain, groundwater on terrain in sewered area, and less than 2 m depth to the phreatic surface) are calculated and shown in table 3.3. Also the results for the median and dry climate scenario are in table 3.3. The results show that all climate scenarios in combination with all hydrological models show an increase in flooding on terrain, as well as flooding of basements. The Storaa and the Dk-model results are somewhat predicting similar floodings, while the Sunds-model is predicting marginally larger areas being affected by future climate induced groundwater flooding. Due to the lack of real observations to compare the predictions with, it is impossible to say which predictions are closest to reality. When comparing the differences, with origin in hydrological model differences, with the differences between climate scenarios, it cannot clearly be stated which is the bigger contributor to the uncertainty of the predictions. Therefore it is not possible to give a clear answer to the research question, if the National Water Resources Model is feasible to use in local scale climate predictions. However, the results show marked differences between the local and the national model scale, which need further investigation to give a finite answer to the research question.

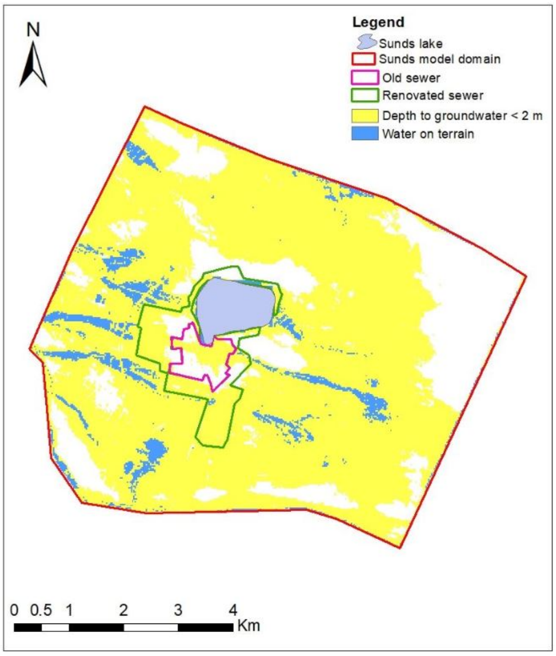

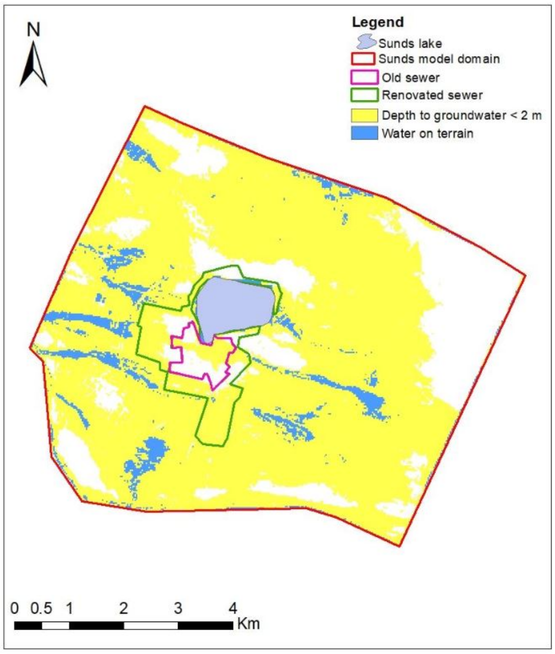

Figure 3.10: The left map shows the area affected by flooding in the future period calculated by the Dk-model and based on the 99 percentile of change in groundwater level computed by the wet climate scenario. The richt map shows the area affected by flooding in the future period calculated by the Storå model and based on the 99 percentile of change in groundwater level computed by the wet climate scenario

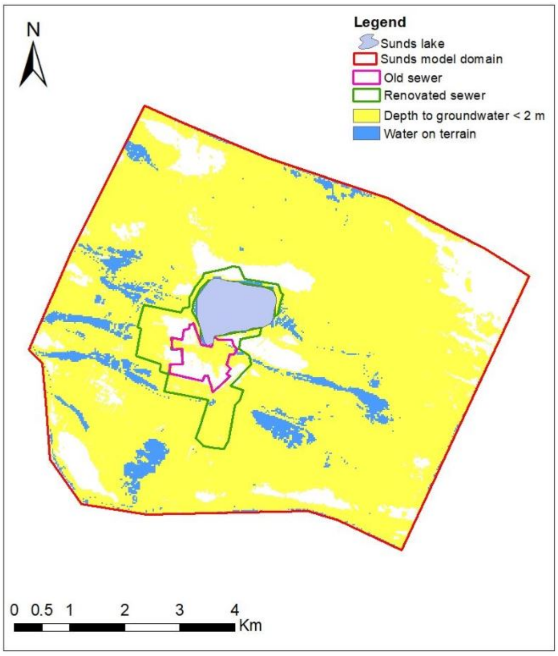

Figure 3.11: This map shows the area affected by flooding in the future period calculated by the Sunds model and based on the 99 percentile of change in groundwater level computed by the wet climate scenario..

Table 3.3: The areas which are affected by future climate scenarios. All areas are calculated in km^2 and based on the 99 percentile for the difference in groundwater level from the present period (1971-2010) to the future period (2071-2100). Terrain = water on terrain, Terrain city = water on terrain in the sewered area, and Basement = depth to shallow groundwater below 2 m.

Flooding	Flooded area	Dk-model	Storå model	Sunds model
Wet climate 99 per.	Terrain	3.86	3.84	4.30
	Terrain city	0.11	0.10	0.12
	Basement	2.10	2.04	2.11
Median climate 99 per.	Terrain	3.11	3.08	3.81
	Terrain city	0.10	0.10	0.11
	Basement	2.01	1.98	2.09
Dry climate 99 per.	Terrain	3.04	2.99	3.61
	Terrain city	0.08	0.07	0.09
	Basement	1.97	1.92	2.04

Chapter 4

Conclusion

Throughout this project, the local scale Sunds model was calibrated to an extent which made it possible to simulate groundwater heads to a satisfactory degree compared to observed values. Three different scaled models were then adjusted to be used in climate predictions for the study site in central Jutland. The three models performed differently when predicting future changes in groundwater levels, it was not possible to trace those differences back to their origin, but based on a superficial water balance analysis, variations in the subsurface flow were identified. Based on the water balance analysis, it is assumed that the updated geology in the Sunds model may be the largest contributor to the differences between the three models. To clarify this, further investigations are required.

The predicted changes in groundwater level were afterwards used to estimate flooding in the area of Sunds. Three climate models, a wet, a median and a dry model were used to predict future groundwater flooding in the area of Sunds. The local model did predict the largest areas exposed to flooding in a future climate. It is to be mentioned that the differences between the three hydrological models is comparable in extend with the difference originating from the climate scenarios. To confirm or deny the use of the Dk-model for local state climate change impact studies, further research needs to be done. Especially detecting and investigating differences in flow pattern between the differently scaled models could give better insight in

More local studies could support the findings of this study and can help understand the relevance of local models when predicting climate change impacts. Especially sites, also known for their problems connected to the shallow groundwater could be used to see if the same tendencies can be observed. The interest in mitigating climate change impacts in the future is steadily growing, and therefore, tools to reliably predicting the impacts of climate change are needed, both on local scale and on a larger scale.

This study gives an insight in the complexity of predicting climate change impacts and how time demanding it can be setting up reliable numerical models which can be used as prediction tools.

Bibliography

[1] John Cappelen. "Danmarks klima 2018 - with English Summary". In: *DMI Report 19-01* (2018).

[2] DHI. "MIKE SHE Volume 1: User Guide". In: (2017).

[3] DHI. "MIKE SHE Volume 2: Reference Guide". In: (2017).

[4] J Doherty. "PEST Model-Independent Parameter Estimation User Manual Part I: PEST". In: *SENSAN and Global Optimiser* (2016).

[5] Miljø og Fødevareministeriet / Miljøstyrelsen. *Klimatipasning*. https://www.klimatilpasning.dk/vae grundvandskort/, 2019.

[6] Hans Jørgen Henriksen et al. "Methodology for construction, calibration and validation of a national hydrological model for Denmark". In: *Journal of Hydrology* 280.1-4 (2003), pp. 52–71.

[7] IPCC. "IPCC special report on renewable energy sources and climate change mitigation". In: (2011).

[8] TAR IPCC. "Climate change 2007: synthesis report". In: *Contribution of working groups I, II and III to the fourth assessment report of the intergovernmental panel on climate change* (2007), pp. 95–212.

[9] Ida Bjørnholt Karlsson et al. "Historical trends in precipitation and stream discharge at the Skjern River catchment, Denmark". In: *Hydrology and Earth System Sciences* 18.2 (2014), p. 595.

[10] Viatcheslav V Kharin et al. "Changes in temperature and precipitation extremes in the IPCC ensemble of global coupled model simulations". In: *Journal of Climate* 20.8 (2007), pp. 1419–1444.

[11] CP Kumar. "Climate change and its impact on groundwater resources". In: *Int J Eng Sci* 1.5 (2012), pp. 43–60.

[12] T Lewis, SA Quinn, and M Hudson. "Potential effects of climate change on water resources in UK sandstone aquifers". In: *European Geosciences Union 1st General Assembly* 6 (2004).

[13] MM Mansour and AG Hughes. "Summary of results for national scale recharge modelling under conditions of predicted climate change". In: (2018).

[14] James J McCarthy et al. *Climate change 2001: impacts, adaptation, and vulnerability: contribution of Working Group II to the third assessment report of the Intergovernmental Panel on Climate Change*. Vol. 2. Cambridge University Press, 2001.

[15] GHP Oude Essink, Esther S Van Baaren, and Perry GB De Louw. "Effects of climate change on coastal groundwater systems: A modeling study in the Netherlands". In: *Water resources research* 46.10 (2010).

[16] Ludovic Oudin et al. "Which potential evapotranspiration input for a lumped rainfall–runoff model?: Part 2—Towards a simple and efficient potential evapotranspiration model for rainfall–runoff modelling". In: *Journal of hydrology* 303.1-4 (2005), pp. 290–306.

[17] Ernesto Pasten-Zapata, Torben O Sonnenborg, and Jens Christian Refsgaard. "Climate change: Sources of uncertainty in precipitation and temperature projections for Denmark". In: *Geological Survey of Denmark and Greenland Bulletin* (2019).

[18] Charles F Pitz. *Predicted impacts of climate change on groundwater resources of Washington State*. Environmental Assessment Program, Washington State Department of Ecology, 2016.

[19] Jens C Refsgaard et al. "Climate change impacts on groundwater hydrology–where are the main uncertainties and can they be reduced?" In: *Hydrological Sciences Journal* 61.13 (2016), pp. 2312–2324.

[20] Jens Christian Refsgaard et al. "God praksis i hydrologisk modellering". In: *GEUS, København* (2010).

[21] Lieke van Roosmalen, Britt SB Christensen, and Torben O Sonnenborg. "Regional differences in climate change impacts on groundwater and stream discharge in Denmark". In: *Vadose Zone Journal* 6.3 (2007), pp. 554–571.

[22] TO Sonnenborg and HJ Henriksen. "Håndbog i grundvandsmodellering". In: *GEUS, København* (2005).

[23] TO Sonnenborg, D Seifert, and JC Refsgaard. "Climate model uncertainty versus conceptual geological uncertainty in hydrological modeling". In: *Hydrology and Earth System Sciences* 19.9 (2015), p. 3891.

[24] Simon Stiesen et al. "National Vandressource Model, Modelopstilling og kalibrering af DK-model 2019". In: (2019).

[25] Ondracek M. Henriksen H. J. Stisen S. Schneider R. J.M. "Modellering af terrænnært grundvand, vandstand i vandløb og vand på terræn for Storå og Odense Å". In: (2018).

[26] Holger Treidel, Jose Luis Martin-Bordes, and Jason J Gurdak. *Climate change effects on groundwater resources: a global synthesis of findings and recommendations*. CRC Press, 2011.

[27] Hydro Geophysics Group Aarhus Universit. *FloaTEM mapping Sunds lake - HydroGeophysics Group*. 2018.

[28] Hydro Geophysics Group Aarhus Universit. *TEM mapping Sunds - HydroGeophysics Group*. 2018.

[29] Detlef P Van Vuuren et al. "The representative concentration pathways: an overview". In: *Climatic change* 109.1-2 (2011), p. 5.

[30] Troels Norvin Vilhelmsen. "Modeling groundwater flow in geological complex areas using local grid refinement, combined parameterization methods, and joint inversion". In: *Aarhus University* (2012).

Appendix A

Observation sensitivities

This appendix holds the calculated sensitivities calculated for each observation. Hts indicates all time series observations, syn indicates the synchronous observation and ho the singe head observations.

Group	Measured	Modelled	Sensitivity
hts_me	0.000000	-0.2990338	35.78387
hts_me	0.000000	-0.2525729	35.56438
hts_me	0.000000	0.1627727	24.65858
hts_me	0.000000	-0.9131538	40.48795
hts_me	0.000000	-0.9331279	21.78039
hts_me	0.000000	1.1113879E-02	41.26216
hts_me	0.000000	-0.2399159	8.124173
hts_me	0.000000	-0.5498086	30.65841
syn_me	0.000000	-0.1124900	9.231077
syn_me	0.000000	-0.2929900	6.683290
syn_me	0.000000	-0.1617200	19.31225
syn_me	0.000000	-0.1185700	11.04003
syn_me	0.000000	-0.2660300	11.89575
syn_me	0.000000	-0.1953300	2.250980
syn_me	0.000000	0.1792800	2.375783
syn_me	0.000000	-7.0450000E-02	14.81852
syn_me	0.000000	3.9560000E-02	2.141868
syn_me	0.000000	-0.1146600	17.50092
syn_me	0.000000	-0.1511000	10.13353
syn_me	0.000000	-5.0060000E-02	6.116741
syn_me	0.000000	0.1723500	6.526556
syn_me	0.000000	0.1691800	2.841889
syn_me	0.000000	-0.2064800	20.60032
syn_me	0.000000	0.1377600	3.815096
syn_me	0.000000	-0.1071300	9.334302
syn_me	0.000000	-0.1190900	8.676863
syn_me	0.000000	0.3644300	18.22804
syn_me	0.000000	8.2720000E-02	0.5211688
syn_me	0.000000	-0.1209100	4.491970
syn_me	0.000000	4.3130000E-02	9.797568
syn_me	0.000000	-1.9900000E-02	8.695179
syn_me	0.000000	0.1316500	2.079655
syn_me	0.000000	0.1565300	16.53333
syn_me	0.000000	0.1995500	13.87719
syn_me	0.000000	9.7640000E-02	1.712574
syn_me	0.000000	7.7870000E-02	0.5635672
syn_me	0.000000	0.3859200	2.684464
syn_me	0.000000	0.2036800	20.59555
syn_me	0.000000	0.1626000	0.8880548
syn_me	0.000000	0.3536000	6.027243
syn_me	0.000000	0.2748600	20.56752
syn_me	0.000000	-3.2880000E-02	21.45507
syn_me	0.000000	-0.3196000	22.32633
syn_me	0.000000	0.1756300	7.858921
syn_me	0.000000	0.2012800	15.48193
syn_me	0.000000	0.3032700	15.19968

syn_me	0.000000	-3.8370000E-02	4.899057
syn_me	0.000000	0.3923700	4.175432
syn_me	0.000000	4.9680000E-02	10.58458
syn_me	0.000000	0.4842000	10.47740
syn_me	0.000000	-9.8290000E-02	2.568537
syn_me	0.000000	0.3564000	5.725929
syn_me	0.000000	0.1465400	16.53675
syn_me	0.000000	-0.1099200	8.695205
syn_me	0.000000	-0.5418600	10.17789
syn_me	0.000000	0.1779600	11.77611
syn_me	0.000000	-8.7620000E-02	11.47123
syn_me	0.000000	-7.0440000E-02	6.356818
syn_me	0.000000	-0.7217500	9.913967
syn_me	0.000000	-0.8071000	6.279123
syn_me	0.000000	-0.7904800	8.945983
syn_me	0.000000	-0.4550400	12.33999
syn_me	0.000000	-0.2583600	16.42054
syn_me	0.000000	-8.5960000E-02	3.201704
syn_me	0.000000	-1.281260	6.611479
syn_me	0.000000	-0.1186100	4.434794
syn_me	0.000000	-0.2156900	14.94032
syn_me	0.000000	0.1284000	12.49474
syn_me	0.000000	0.1249200	13.51572
syn_me	0.000000	0.1014100	22.76417
syn_me	0.000000	5.2140000E-02	0.9014437
syn_me	0.000000	-0.1050100	12.57403
syn_me	0.000000	1.124000	5.547333
syn_me	0.000000	-3.4850000E-02	3.194876
syn_me	0.000000	0.1994000	5.655725
ho_me	0.000000	-1.274720	0.6499831
ho_me	0.000000	-0.4211100	3.156053
ho_me	0.000000	-0.3833000	7.206992
ho_me	0.000000	-1.290820	6.986065
ho_me	0.000000	0.1519500	4.403830
ho_me	0.000000	1.243370	8.912075
ho_me	0.000000	-0.1201000	0.1987097
ho_me	0.000000	-0.1023800	1.891209
ho_me	0.000000	-0.9837200	9.668434
ho_me	0.000000	-9.3540000E-02	2.491991
ho_me	0.000000	-1.281710	4.046798
ho_me	0.000000	-0.1592100	3.727025
ho_me	0.000000	-1.339080	6.968964
ho_me	0.000000	0.1864600	2.491991
ho_me	0.000000	1.118110	1.296276
ho_me	0.000000	0.1164600	2.491991
ho_me	0.000000	0.1567000	7.305229
ho_me	0.000000	-0.1866000	9.794648

ho_me	0.000000	-2.012360	1.300992
ho_me	0.000000	0.3036900	8.022746
ho_me	0.000000	-0.6467500	4.882100
ho_me	0.000000	-1.419420	6.088508
ho_me	0.000000	-3.102750	3.959110
ho_me	0.000000	-0.3990700	9.131792
ho_me	0.000000	-0.3910500	5.808881
ho_me	0.000000	-0.4432800	7.894989
ho_me	0.000000	-1.158600	3.524498
ho_me	0.000000	9.3060000E-02	1.786259
ho_me	0.000000	-0.3236400	7.112061
ho_me	0.000000	-1.280470	0.8011413
ho_me	0.000000	-0.7069900	2.624489
ho_me	0.000000	-0.3951700	8.011570
ho_me	0.000000	-0.5245400	4.369730
hts_errampl	0.000000	0.1046150	77.37985
hts_errampl	0.000000	0.1649054	109.7068
hts_errampl	0.000000	0.1276190	99.16767
hts_errampl	0.000000	3.0962000E-02	107.0326
hts_errampl	0.000000	-0.2252357	114.2382
hts_errampl	0.000000	-0.1191300	65.74644
hts_errampl	0.000000	4.8294333E-02	68.35941
hts_errampl	0.000000	9.8144636E-02	51.43184

Appendix B

Calibration Log

This appendix holds the calibration log including the estimated parameters during each interation.

```
OPTIMISATION ITERATION NO.        : 1
   Model calls so far             : 1
   Starting phi for this iteration                          :   101.44
   Contribution to phi from observation group "hts_me"      :   35.340
   Contribution to phi from observation group "hts_errampl" :   30.706
   Contribution to phi from observation group "syn_me"      :   20.264
   Contribution to phi from observation group "ho_me"       :   15.131
       param "khl_hc" frozen: gradient and update vectors out of bounds

       Lambda =   5.0000    ----->
          Phi =   97.923      (  0.965 of starting phi)

       Lambda =   2.5000    ----->
          Phi =   97.728      (  0.963 of starting phi)

   No more lambdas: relative phi reduction between lambdas less than 0.0100
   Lowest phi this iteration:   97.728
   Relative phi reduction between optimisation iterations less than 0.0500
   Switch to higher order derivatives calculation

      Current parameter values                 Previous parameter values
      gp_hc          4.629500E-06              gp_hc          5.180000E-06
      wsds_hc        1.067847E-04              wsds_hc        1.000000E-04
      wsdg_hc        1.000000E-04              wsdg_hc        1.000000E-04
      ksmw_hc        5.075358E-05              ksmw_hc        5.000000E-05
      kl_hc          6.655523E-06              kl_hc          6.220000E-06
      klmw_hc        6.655523E-07              klmw_hc        6.220000E-07
      kgmw_hc        1.000000E-04              kgmw_hc        1.000000E-04
      ksbw1_hc       9.967663E-05              ksbw1_hc       1.000000E-04
      ksbw2_hc       1.000000E-04              ksbw2_hc       1.000000E-04
      mgc_hc         2.834575E-07              mgc_hc         2.800000E-07
      kso_hc         2.020000E-04              kso_hc         2.020000E-04
      al_hc          2.581105E-07              al_hc          2.800000E-07
      gso_hc         4.867403E-05              gso_hc         4.620000E-05
      ksb_hc         4.040000E-04              ksb_hc         4.040000E-04
      gsb_hc         4.888474E-05              gsb_hc         4.640000E-05
      khl_hc         1.000000E-10              khl_hc         1.000000E-10
      bs_hc          1.000000E-04              bs_hc          1.000000E-04
      vf_hc          1.000000E-04              vf_hc          1.000000E-04
      mios_hc        1.000000E-04              mios_hc        1.000000E-04
      gp_vc          4.629500E-07              gp_vc          5.180000E-07
      wsds_vc        1.067847E-05              wsds_vc        1.000000E-05
      wsdg_vc        1.000000E-05              wsdg_vc        1.000000E-05
      ksmw_vc        5.075358E-06              ksmw_vc        5.000000E-06
      kl_vc          6.655523E-07              kl_vc          6.220000E-07
      klmw_vc        6.655523E-08              klmw_vc        6.220000E-08
      kgmw_vc        1.000000E-05              kgmw_vc        1.000000E-05
```

ksbw1_vc	9.967663E-06	ksbw1_vc	1.000000E-05
ksbw2_vc	1.000000E-05	ksbw2_vc	1.000000E-05
mgc_vc	2.834575E-08	mgc_vc	2.800000E-08
kso_vc	2.020000E-05	kso_vc	2.020000E-05
al_vc	2.581105E-08	al_vc	2.800000E-08
gso_vc	4.867403E-06	gso_vc	4.620000E-06
ksb_vc	4.040000E-04	ksb_vc	4.040000E-04
gsb_vc	4.867403E-05	gsb_vc	4.620000E-05
khl_vc	1.000000E-10	khl_vc	1.000000E-10
bs_vc	1.000000E-05	bs_vc	1.000000E-05
vf_vc	1.000000E-05	vf_vc	1.000000E-05
mios_vc	1.000000E-05	mios_vc	1.000000E-05
gp_sy	0.200000	gp_sy	0.200000
wsds_sy	0.283772	wsds_sy	0.300000
wsdg_sy	0.300000	wsdg_sy	0.300000
ksmw_sy	0.283772	ksmw_sy	0.300000
kl_sy	5.000000E-02	kl_sy	5.000000E-02
klmw_sy	5.000000E-02	klmw_sy	5.000000E-02
kgmw_sy	0.300000	kgmw_sy	0.300000
ksbw1_sy	0.283772	ksbw1_sy	0.300000
ksbw2_sy	0.300000	ksbw2_sy	0.300000
mgc_sy	5.000000E-02	mgc_sy	5.000000E-02
kso_sy	0.300000	kso_sy	0.300000
al_sy	5.000000E-02	al_sy	5.000000E-02
gso_sy	0.300000	gso_sy	0.300000
ksb_sy	0.300000	ksb_sy	0.300000
gsb_sy	0.300000	gsb_sy	0.300000
khl_sy	5.000000E-02	khl_sy	5.000000E-02
bs_sy	0.300000	bs_sy	0.300000
vf_sy	0.300000	vf_sy	0.300000
mios_sy	0.300000	mios_sy	0.300000
gp_ss	1.000000E-04	gp_ss	1.000000E-04
wsds_ss	1.000000E-04	wsds_ss	1.000000E-04
wsdg_ss	1.000000E-04	wsdg_ss	1.000000E-04
ksmw_ss	1.000000E-04	ksmw_ss	1.000000E-04
kl_ss	1.000000E-04	kl_ss	1.000000E-04
klmw_ss	1.000000E-04	klmw_ss	1.000000E-04
kgmw_ss	1.000000E-04	kgmw_ss	1.000000E-04
ksbw1_ss	1.000000E-04	ksbw1_ss	1.000000E-04
ksbw2_ss	1.000000E-04	ksbw2_ss	1.000000E-04
mgc_ss	1.000000E-04	mgc_ss	1.000000E-04
kso_ss	1.076118E-04	kso_ss	1.000000E-04
al_ss	1.000000E-04	al_ss	1.000000E-04
gso_ss	1.076118E-04	gso_ss	1.000000E-04
ksb_ss	1.076118E-04	ksb_ss	1.000000E-04
gsb_ss	1.076118E-04	gsb_ss	1.000000E-04
khl_ss	1.000000E-04	khl_ss	1.000000E-04

```
     bs_ss           1.000000E-04             bs_ss            1.000000E-04
     vf_ss           1.000000E-04             vf_ss            1.000000E-04
     mios_ss         1.000000E-04             mios_ss          1.000000E-04
     draints         1.260000E-07             draints          1.260000E-07
     pdin_ts         9.508783E-04             pdin_ts          1.000000E-03
     pdout_ts        9.508783E-04             pdout_ts         1.000000E-03
     l_sunds         9.888173E-07             l_sunds          1.000000E-06
     l_moel          2.410000E-05             l_moel           2.410000E-05
   Maximum   factor change:  1.119     ["gp_hc"]
   Maximum relative change: 0.1063     ["gp_hc"]


OPTIMISATION ITERATION NO.        : 2
   Model calls so far             : 16
   Starting phi for this iteration                         :   97.728
   Contribution to phi from observation group "hts_me"      :   34.452
   Contribution to phi from observation group "hts_errampl" :   28.620
   Contribution to phi from observation group "syn_me"      :   19.837
   Contribution to phi from observation group "ho_me"       :   14.819
   All frozen parameters freed.

       Lambda =   1.2500     ----->
          Phi =   72.799      (  0.745 of starting phi)

       Lambda =  0.62500     ----->
          Phi =   72.683      (  0.744 of starting phi)

   No more lambdas: relative phi reduction between lambdas less than 0.0100
   Lowest phi this iteration:   72.683

     Current parameter values                 Previous parameter values
     gp_hc           3.968397E-06             gp_hc            4.629500E-06
     wsds_hc         2.423478E-04             wsds_hc          1.067847E-04
     wsdg_hc         1.000000E-04             wsdg_hc          1.000000E-04
     ksmw_hc         3.138305E-05             ksmw_hc          5.075358E-05
     kl_hc           4.794004E-06             kl_hc            6.655523E-06
     klmw_hc         4.794004E-07             klmw_hc          6.655523E-07
     kgmw_hc         1.000000E-04             kgmw_hc          1.000000E-04
     ksbw1_hc        1.113221E-04             ksbw1_hc         9.967663E-05
     ksbw2_hc        1.000000E-04             ksbw2_hc         1.000000E-04
     mgc_hc          2.062320E-07             mgc_hc           2.834575E-07
     kso_hc          2.020000E-04             kso_hc           2.020000E-04
     al_hc           2.318582E-07             al_hc            2.581105E-07
     gso_hc          5.864001E-05             gso_hc           4.867403E-05
     ksb_hc          4.040000E-04             ksb_hc           4.040000E-04
     gsb_hc          5.889386E-05             gsb_hc           4.888474E-05
     khl_hc          1.235909E-10             khl_hc           1.000000E-10
```

bs_hc	1.000000E-04	bs_hc	1.000000E-04
vf_hc	1.000000E-04	vf_hc	1.000000E-04
mios_hc	1.000000E-04	mios_hc	1.000000E-04
gp_vc	3.968397E-07	gp_vc	4.629500E-07
wsds_vc	2.423478E-05	wsds_vc	1.067847E-05
wsdg_vc	1.000000E-05	wsdg_vc	1.000000E-05
ksmw_vc	3.138305E-06	ksmw_vc	5.075358E-06
kl_vc	4.794004E-07	kl_vc	6.655523E-07
klmw_vc	4.794004E-08	klmw_vc	6.655523E-08
kgmw_vc	1.000000E-05	kgmw_vc	1.000000E-05
ksbw1_vc	1.113221E-05	ksbw1_vc	9.967663E-06
ksbw2_vc	1.000000E-05	ksbw2_vc	1.000000E-05
mgc_vc	2.062320E-08	mgc_vc	2.834575E-08
kso_vc	2.020000E-05	kso_vc	2.020000E-05
al_vc	2.318582E-08	al_vc	2.581105E-08
gso_vc	5.864001E-06	gso_vc	4.867403E-06
ksb_vc	4.040000E-04	ksb_vc	4.040000E-04
gsb_vc	5.864001E-05	gsb_vc	4.867403E-05
khl_vc	1.235909E-10	khl_vc	1.000000E-10
bs_vc	1.000000E-05	bs_vc	1.000000E-05
vf_vc	1.000000E-05	vf_vc	1.000000E-05
mios_vc	1.000000E-05	mios_vc	1.000000E-05
gp_sy	0.200000	gp_sy	0.200000
wsds_sy	0.222144	wsds_sy	0.283772
wsdg_sy	0.300000	wsdg_sy	0.300000
ksmw_sy	0.222144	ksmw_sy	0.283772
kl_sy	5.000000E-02	kl_sy	5.000000E-02
klmw_sy	5.000000E-02	klmw_sy	5.000000E-02
kgmw_sy	0.300000	kgmw_sy	0.300000
ksbw1_sy	0.222144	ksbw1_sy	0.283772
ksbw2_sy	0.300000	ksbw2_sy	0.300000
mgc_sy	5.000000E-02	mgc_sy	5.000000E-02
kso_sy	0.300000	kso_sy	0.300000
al_sy	5.000000E-02	al_sy	5.000000E-02
gso_sy	0.300000	gso_sy	0.300000
ksb_sy	0.300000	ksb_sy	0.300000
gsb_sy	0.300000	gsb_sy	0.300000
khl_sy	5.000000E-02	khl_sy	5.000000E-02
bs_sy	0.300000	bs_sy	0.300000
vf_sy	0.300000	vf_sy	0.300000
mios_sy	0.300000	mios_sy	0.300000
gp_ss	1.000000E-04	gp_ss	1.000000E-04
wsds_ss	1.000000E-04	wsds_ss	1.000000E-04
wsdg_ss	1.000000E-04	wsdg_ss	1.000000E-04
ksmw_ss	1.000000E-04	ksmw_ss	1.000000E-04
kl_ss	1.000000E-04	kl_ss	1.000000E-04
klmw_ss	1.000000E-04	klmw_ss	1.000000E-04

```
     kgmw_ss         1.000000E-04             kgmw_ss          1.000000E-04
     ksbw1_ss        1.000000E-04             ksbw1_ss         1.000000E-04
     ksbw2_ss        1.000000E-04             ksbw2_ss         1.000000E-04
     mgc_ss          1.000000E-04             mgc_ss           1.000000E-04
     kso_ss          6.627483E-05             kso_ss           1.076118E-04
     al_ss           1.000000E-04             al_ss            1.000000E-04
     gso_ss          6.627483E-05             gso_ss           1.076118E-04
     ksb_ss          6.627483E-05             ksb_ss           1.076118E-04
     gsb_ss          6.627483E-05             gsb_ss           1.076118E-04
     khl_ss          1.000000E-04             khl_ss           1.000000E-04
     bs_ss           1.000000E-04             bs_ss            1.000000E-04
     vf_ss           1.000000E-04             vf_ss            1.000000E-04
     mios_ss         1.000000E-04             mios_ss          1.000000E-04
     draints         1.260000E-07             draints          1.260000E-07
     pdin_ts         1.479744E-03             pdin_ts          9.508783E-04
     pdout_ts        1.479744E-03             pdout_ts         9.508783E-04
     l_sunds         1.940345E-06             l_sunds          9.888173E-07
     l_moel          2.410000E-05             l_moel           2.410000E-05
   Maximum   factor change:  2.269     ["wsds_hc"]
   Maximum relative change:  1.269     ["wsds_hc"]


OPTIMISATION ITERATION NO.        : 3
   Model calls so far             : 50
   Starting phi for this iteration                          :   72.683
   Contribution to phi from observation group "hts_me"      :   21.788
   Contribution to phi from observation group "hts_errampl" :   16.996
   Contribution to phi from observation group "syn_me"      :   21.715
   Contribution to phi from observation group "ho_me"       :   12.185
```

Appendix C

Water Balance Plots

This appendix holds the water balance graphs for the 3 models.

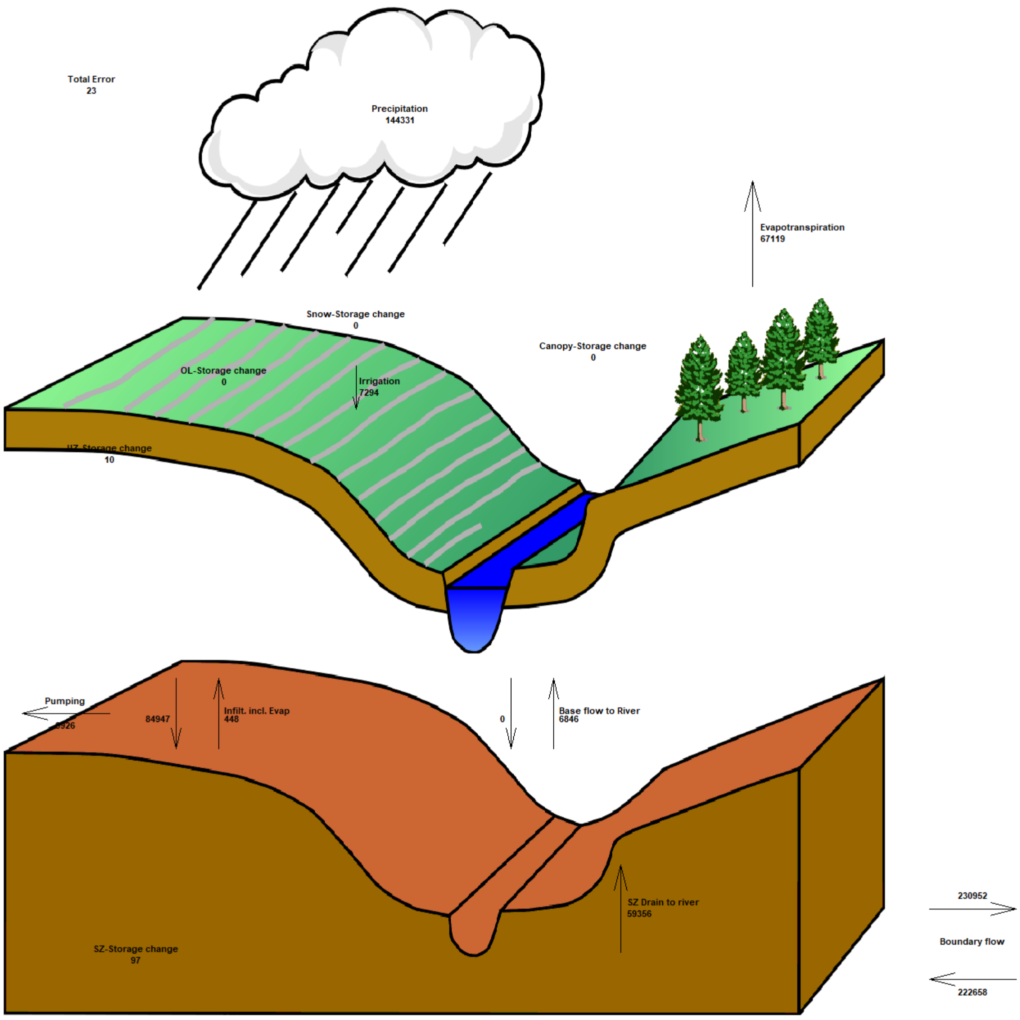

Figure C.1: Waterbalance for the Dk-Model.

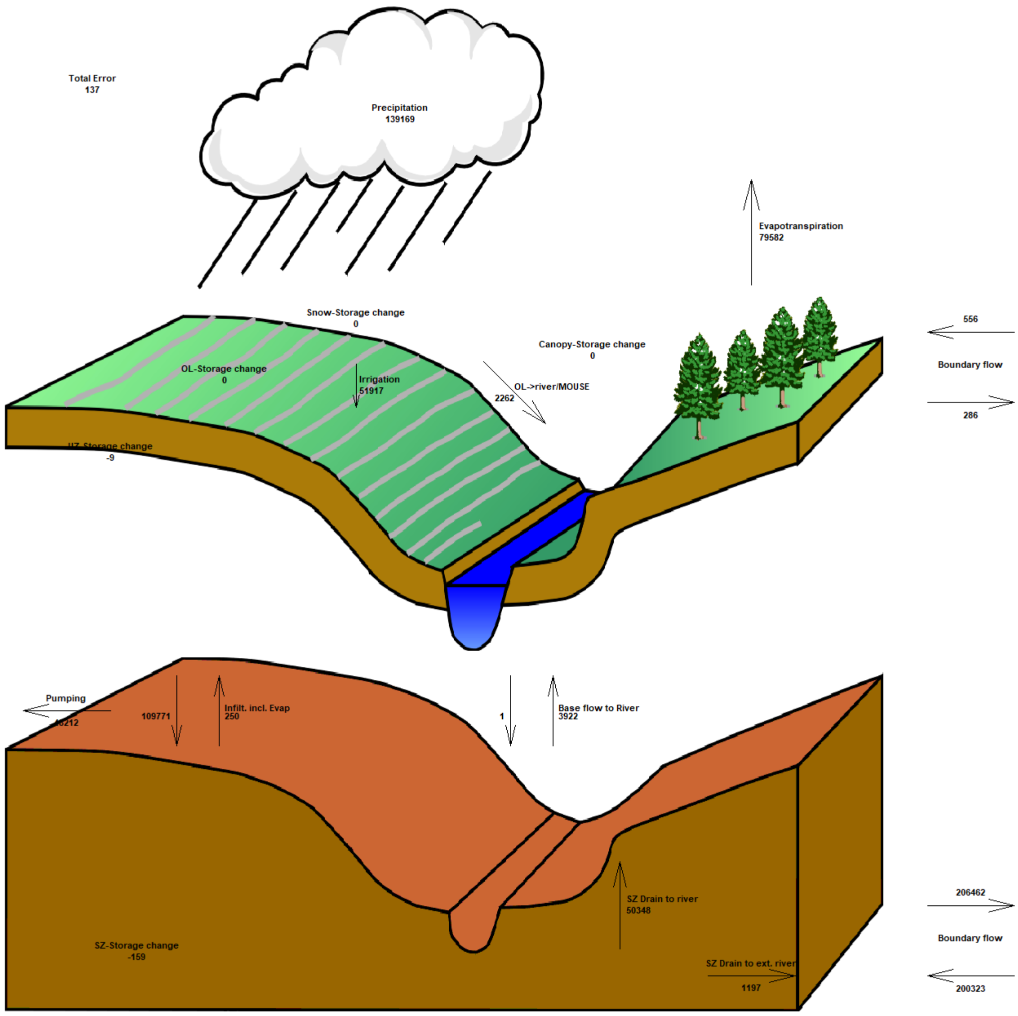

Figure C.2: Waterbalance for the Storå Model.

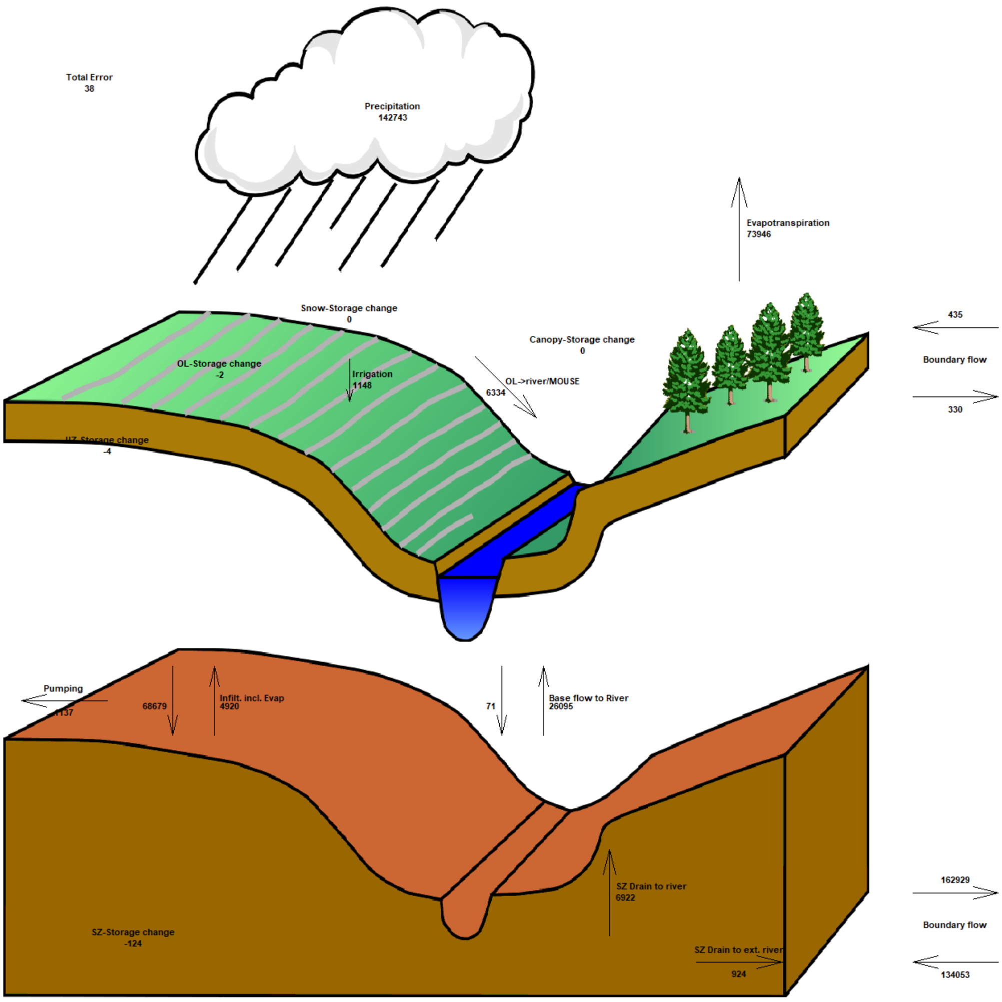

Figure C.3: Waterbalance for the Sunds Model.